geographies

MDPI

Article

Spatiotemporal Study of Land Degradation Impacting the Oldest Mountains of the Indian Subcontinent

Rahul Devrani [1,*], Rohit Kumar [1], Jitendra Kumar Roy [2] and Abhiroop Chowdhury [1,*]

[1] Jindal School of Environment & Sustainability, O.P Jindal Global University, Sonipat 131001, Haryana, India
[2] Department of Geology and Geophysics, Indian Institute of Technology Kharagpur, Kharagpur 721302, West Bengal, India
* Correspondence: rahuldevrani18@gmail.com (R.D.); abhiroop.chowdhury@gmail.com (A.C.)

Abstract

The Aravalli Mountain System (AMS) is one of the oldest fold orogens in the world, serving as a natural boundary against desertification in north-western India. The AMS has high environmental importance and faces accelerated soil degradation driven by both anthropogenic pressures and climatic shifts. Still, high-resolution measurements of soil erosion processes have not been conducted on the AMS scale. The present study assesses long-term LULC transitions between 2001 and 2021, identifies high-resolution short-term LULC dynamics between 2017 and 2024, and models spatiotemporal soil erosion dynamics using the RUSLE model. The findings indicate that LULC has changed rapidly, with built-up areas increasing by 53 per cent at the expense of rangelands and croplands. These drivers resulted in a 13.8 per cent increase in the mean annual soil loss between 2017 and 2024, from 1.59 to 1.81 t/ha/yr, while forest cover has increased over the timescale, as is evident in this study. The steep slopes, susceptible soils, and mining areas are strongly associated with erosion hotspots. Increased soil erosion in the AMS despite a significant increase in afforestation highlights that local conservation cannot compensate for massive land conversion. The present study provides a scalable, high-resolution framework for assessing soil erosion in vulnerable old mountain systems globally for sustainable land-use planning, mineral governance, and integrated conservation to protect for future generations.

Keywords: land degradation; RUSLE; Aravalli Mountain System; soil erosion; mining impact

1. Introduction

Land degradation is one of the critical Anthropocene environmental dilemmas that threatens ecosystems, biodiversity, and human livelihoods on a global scale [1]. The problem is acute in ancient, tectonically stable mountain systems, where billions of years of geomorphic activity have produced subdued topography, deeply weathered soils, and venerable balanced ecosystems [2]. Soil erosion, a significant aspect of land degradation, is a pronounced phenomenon in these mountain systems, strongly influenced by the complex interplay between land cover dynamics and land use change, such as deforestation, agricultural expansion, urbanization, mining, and unsustainable land management practices [3–5]. Their structural stability and natural resource endowment often make them susceptible to persistent anthropogenic stressors, including unsustainable agricultural intensification, unregulated mining/quarrying, explosive urban growth, concretization, and biomass extraction [6]. These changes in land use and land cover (LULC) destabilize sensitive ecological balances through the loss of protective vegetation, disruption of soil structure, and

Academic Editor: Pedro Cabral

Received: 17 January 2026
Revised: 27 February 2026
Accepted: 3 March 2026
Published: 6 March 2026

altered hydrological regimes, thereby leading to significant increases in sediment yields, reductions in soil fertility, and the loss of ecosystem services [3,7]. The dynamics of land degradation thus require a combined approach that integrates LULC analysis with soil erosion modeling, a methodology that has been demonstrated to be highly effective in scores of studies worldwide [4].

These interventions disrupt the native vegetation, cause physical and chemical changes in the soil, and enhance soil erosion rates, leading to low land productivity, loss of biodiversity, and increased vulnerability to natural hazards [3]. Understanding the land degradation process through simultaneous assessment of LULC changes and soil erosion processes is therefore an essential step in developing effective conservation and restoration programs that protect the ecosystem services and strengthen the livelihoods [8]. In the Appalachian Mountains of the United States, researchers have used satellite-derived LULC maps with the Revised Universal Soil Loss Equation (RUSLE) to quantify increased sediment yields attributable to historical deforestation and surface mining [9]. Similar integrative frameworks have been used in the Mediterranean basin of ancient mountain systems in Spain and Italy to evaluate the role of abandonment of traditional terraced agriculture and vegetation succession in creating non-linear patterns of erosion risk (and, conversely, the intensification of certain types of cultivation) [10]. Coupled LULC change and erosion modeling analyses have become indispensable in the highlands of East Africa and the Andes for establishing relationships between the growth of subsistence agriculture on steep slopes, visible erosion, and the decline of food security [11,12]. Such studies suggest that combining LULC and soil erosion analyses can provide not only descriptive assessments of the landscape but also a quantitative diagnostic instrument that shifts the focus from observing symptoms to explaining processes. Such an integrated approach will provide a sound scientific basis for the development of specific sustainable land restoration policies by identifying key anthropogenic drivers and predicting the future under different socio-economic and climatic pathways.

Recent geospatial techniques used in the semi-arid region of western India have estimated land degradation, LULC changes, and the rate of soil erosion, which are not only the result of physical processes but also reflect the effects of climate change on the geomorphology that drives erosion [11]. Many studies use RUSLE, Google Earth Engine, at watershed, basin scales, or very subwatershed scales to estimate the soil erosion areas adjacent to Aravalli, the Chambal basin, the Indo-Gangetic plain, and the Rajasthan and Gujarat River basin, which indicate a higher rate of erosion in barren, geologically active regions and hills [7,12–14]. Many studies have used AHP, fuzzy methods, some machine learning models, and CART-based LULC to identify hotspots of higher erosion rates more accurately [15–18]. Many studies focus on LULC dynamics that reveal the conversion of forest and scrubland to agricultural use or urban expansion, which has reduced the barrier between soil and surface runoff, leading to higher erosion rates [19–21]. Further studies on strategic environmental assessment and geoheritage evaluation suggest that ravine degradation and the development of barren land are associated with higher erosion rates [19,22,23]. Research on gully area mapping that causes higher rates of erosion, desertification, abiotic stress mapping, and climate-driven degradation indicates that climate change directly affects geomorphic processes and causes land degradation [5,15,24,25].

An example of this global phenomenon is the Aravalli Mountain System (AMS), an ancient system of folds of global interest that has experienced significant land degradation in the last decades [26]. The Aravalli acts as a natural barrier limiting the eastern transgression of the Thar Desert, serves as the principal groundwater recharge area to north-western India, and is home to distinct fauna and flora. However, in recent decades, rapid urbanization, deforestation, agricultural expansion, and unsustainable mining ac-

tivities have promoted land degradation and adversely affected the ecological balance, groundwater recharge, and socio-economic interests [27,28]. Despite the environmental and socio-economic significance of the AMS and its role in influencing the meteorological conditions of India, quantitative assessments linking LULC change with soil erosion dynamics remain limited [29–31], though broader studies are available [32]. Beyond biophysical drivers, policy and governance play a critical role in shaping LULC dynamics in any region. Recent policy developments may have consequences for the Aravalli system. The future of the Aravalli range is an issue of national importance, and the Honourable Supreme Court of India deliberated on redefining the geographical scope of the range, which spans many Indian states. The ruling was issued on 20 November 2025 and was based on the classification of the hills, primarily by altitude, which limited legal protection to locations above the 100-meter contour line. Environmental groups call this a narrow definition, which may leave almost 90% of the land unprotected, according to some opinions. This may arguably alter existing land use patterns. There are also concerns among some environmental groups about potential unregulated mining in the ecologically sensitive Aravalli landscape [33]. Instead of direct implementation, the Court has suggested the creation of a top expert board whose duty would be to carry out a thorough examination of the matter [34]. Comprehensive scientific studies are needed in the region, given recent developments, to facilitate informed policymaking. This research sought to address some of the policy gaps by developing a scientific understanding of the concerns (soil erosion, land degradation, and forest cover) surrounding the conservation of the AMS.

This future report of the high-level committee on the Aravalli system will play a vital role in defining the Aravalli system in Indian states, making the future of the Aravalli a subject of active debate. The new definition will decide the future mining activities in the region. The implications of this judicial ruling for the AMS are discussed in detail in the Section 4. Rapid urbanization, especially driven by the explosive development of metropolitan areas, the intensive extraction of marble and granite, deforestation, and land fragmentation have led to significant and even irreversible changes in land cover [35]. These alterations have increased erosion in sheet, rill, and gullies, leading to siltation of important reservoirs, reduced agricultural output, and reduced groundwater recharge [36]. As a result, the geographically defined and scientifically rigorous application of an internationally recognized, combined LCLU–soil erosion methodology (RUSLE) to the Aravalli is critical. This initiative is a unique chance to determine the clear degradation routes in this highly threatened ancient system, thus producing data and knowledge that can be applied to conservation efforts in the AMS and contribute to how to proceed with such a sensitive landscape. Therefore, in the present study, the main objectives are to detect long-term LULC change (2001 to 2021) from MODIS, detect high-resolution short-term LULC dynamics (2017 to 2024), and predict the rate of soil erosion (a major aspect of land degradation) dynamics in 2017 and 2024 using the RUSLE Model at 30 m spatial resolution for the first time on an AMS scale. This will be the first attempt at such studies on the AMS scale.

2. Materials and Methods

2.1. Overview of Study Area

The AMS of India includes the Caledonian mountains of the old Palaeozoic and Mesozoic era that are now just deeply eroded remnants due to very long and repeated erosion cycles [15–18]. This study focused on the AMS region, extended to Rajasthan, Haryana, Gujarat, and Delhi (Figure 1). The spatial extent of the Aravalli Mountain System (AMS) remains variably defined across institutional datasets. The Geological Survey of India (GSI) delineates the Aravalli range based on lithological, structural, and tectonic criteria. In contrast, the Survey of India provides only topographic representations without an official

geomorphic or geological boundary. Consequently, no universally accepted methodology currently exists for AMS boundary demarcation. In this study, the AMS extent has therefore been defined based on available literature sources [15,16,18,29]. In the absence of any acceptable boundary, this is the only method available to us, to the best of our knowledge, to execute this study. This is also the limitation of this study. The area is bounded between 23.82 and 28.66 latitudes and 72.312 and 77.31 longitudes with a mean height of 400.04 m. It includes older alluvium (32,495.9 km^2), the Thar Desert (19,603.6 km^2), Kumbhalgarh (5153.32 km^2), Gogunda (2960.44 km^2), Alwar (2545.55 km^2), Sandmata (2325.94 km^2), jharol (2248.56 km^2), Ajabgarh (2122.17 km^2), Mangalwar (1540.58 km^2), Sirohi (1008.73 km^2), Udaipur (967.287 km^2), and other small groups or sub-groups of Debari, Dovda, Raialo, Bari Lake, Kankroli, etc. (https://bhukosh.gsi.gov.in; (accessed on 4 January 2026) [26]). Geomorphologically, the area comprises a pediment pediplain complex (32,370.6 km^2), aeolian sand sheet (9751.42 km^2), highly dissected structural hills and valleys (8828.68 km^2), moderately dissected structural hills and valleys (6497.6 km^2), alluvial plains (5064.93 km^2), aeolian plains (4163.61 km^2), dunes (2605.88 km^2), waterbodies (1430.14 km^2), aeolian dune complexes (1061.89 km^2), moderately dissected denudational hills and valleys (988.665 km^2), low dissected structural hills and valleys (765.029 km^2), active flood plains (671.315 km^2), highly dissected denudational hills and valleys (583.012 km^2), aeolian dissected dune complexes (364.407 km^2), and playa (316.906 km^2), with some active quarry (121.245 km^2) (https://bhukosh.gsi.gov.in (accessed on 4 January 2026)). This active quarry indicates that mining continues in many places across the Aravalli region.

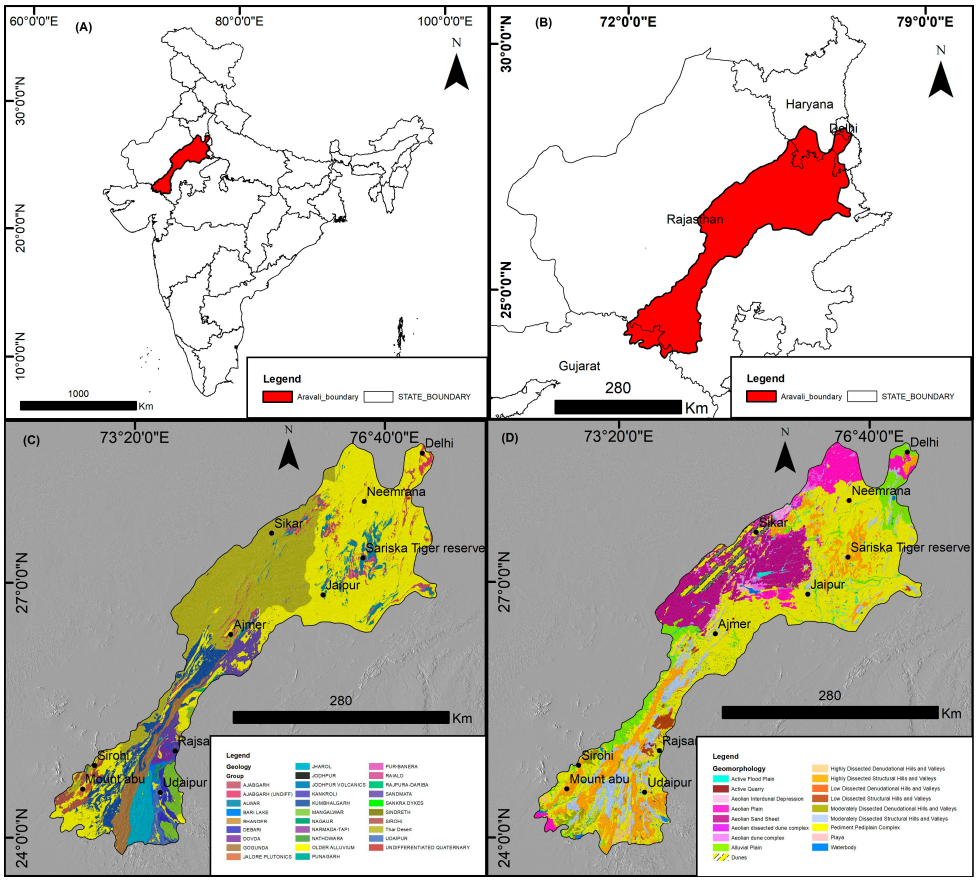

Figure 1. Location map of the study area. (**A**) The spatial distribution of the Aravalli region, draped over the Indian boundary. (**B**) Greater detail of the Indian state boundary to highlight the state covered by the Aravalli region. (**C**) The geology of the Aravalli region highlighted draped over hillshade. (**D**) The geomorphic units, showing the dominance of pediment pediplain complexes and aeolian sand sheet draped over hillshade.

The Aravalli Mountain System is one of India's most mineral-rich mountain systems, characterized by a complex geological history involving many periods of deformation, sedimentation, metamorphism, and polyphase granitic magmatism. These complex geological processes resulted in a structurally intricate and lithologically diverse crust. As a result, the region hosts a wide spectrum of metallic and non-metallic mineral systems and serves as a cornerstone of India's mineral resource base.

2.2. Data and Its Analysis

The study area is the main core of the Aravalli Mountain System in North India. A thorough analysis was conducted from 2001 to 2020 using moderate-resolution data to identify long-term trends. To accurately measure erosion trends, two years were selected at high resolution, 2017 and 2024, which represent the current and divergent meteorological conditions. The fact that the Aravalli mountains are among the world's oldest fold mountains demonstrates how vulnerable stable, eroded landscapes are to human-induced changes. These are primitive mountains where the soils are deep and the ecosystems are intricate and in a delicate balance. Mostly, accelerated deterioration is not the result of sudden natural events but the result of long-term human activity. The most significant processes are changes in land use and land cover (LULC) through urban development, mining, deforestation, and agricultural intensification, which directly affect two key erosion controls: the vegetation canopy (C factor) and land management practices (P factor). It is within this context that this framework places the Aravalli case in the world context where similar studies in the Appalachians, the Mediterranean highlands, and the Andes have always used a combination of land use and land cover (LULC) analysis with erosion modeling (e.g., RUSLE) to determine the pathways of degradation where the observation of degradation is replaced by the quantification process-based analysis.

For long-term analysis, we first procured the MODIS LULC data for 2001, 2010, and 2020 to analyze spatial variation in the Aravalli range over 20 years (MODIS LULC = MODIS/006/MCD12Q1) (for details regarding the classification of the MODIS LULC, please refer to Supplementary S4). ESRI Land cover (10 m resolution) was used to accurately identify the change and the parameterization of the erosion factor between the years 2017 and 2024. The ALOS PALSAR Digital Elevation Model (DEM) at 30 m resolution was mosaiced and processed to obtain slope length and steepness (LS factor). The 2017 and 2024 rainfall data, at a resolution of approximately 4 km in the CHRS Data Portal, was spatially refined using 30 m Inverse Distance Weighting (IDW) interpolation (the Aravalli Mountain System is characterized by complex topography and spatial distribution may be affected by orographic effects, but due to non-availability of high-resolution data or region-specific data, we have used 4 km spatial resolution data). In this study, we have not used a direct downscaling tool, e.g., Raster resampling or Warp, due to uncertainty, e.g., smoothing effects and pixel duplication associated with it. Our methodology involves reprojection of CHRS rainfall data into UTM43 then converting the raster data to point data. Inverse Distance Weighting (IDW) is used to interpolate because it uses each point's distance to the point of interest, meaning each value is determined by nearby points. Furthermore, 30 m cell size was given as the output cell size in IDW interpolation. Although IDW is widely used, it has some limitations: it does not use a spatial autocorrelation statistical model (deterministic method), and it is sensitive to data density. With fewer points, it has lower accuracy; with more points, it has higher accuracy.

We used Sentinel-2 to determine the Normalized Difference Vegetation Index (NDVI) of pre- and post-monsoon seasons of 2017–2024. Soil texture maps from the National Bureau of Soil Survey and Land Use Planning (NBSS and LUP) were used to assign erodibility (K factor) values. The details for each dataset are given in the in Supplementary S4.

2.3. Land Use and Land Cover (LULC) Change Analysis

The datasets were created to detect changes (e.g., forest, cropland, rangeland, built-up) by generating change detection matrices using MODIS (2001–2020) and ESRI (2017–2024) data. This ESRI categorization at high resolution was necessary to identify subtle landscape changes not visible in the coarse data, such as rangeland fragmentation and small-scale mining, which are significant local sources of degradation.

2.4. Simulating Soil Erosion Using the Revised Universal Soil Loss Equation (RUSLE)

The loss of soil (A in t ha^{-1} yr^{-1}) was determined utilizing the RUSLE, which takes into consideration climatic, topographic, edafic, and anthropogenic factors:

$$A = R \times K \times L \times S \times C \times P \quad (1)$$

where A is the annual rate of soil loss, R is rainfall erosivity, K is soil erodibility, L is slope length, S is slope steepness, C is crop management, and P is crop support factor.

We are calculating the RUSLE for two time intervals; therefore, the RUSLE formula can be rewritten as

$$A = R\ \text{variable} \times K\ \text{constant} \times L\ \text{constant} \times S\ \text{constant} \times C\ \text{variable} \times P\ \text{variable} \quad (2)$$

where A is the annual rate of soil loss, R is rainfall erosivity, K is soil erodibility, L is slope length, S is slope steepness, C is crop management, and P is crop support factor. Variable factors will change with time, and constant variables will remain the same. The factors were acquired in the following way:

- *Rainfall Erosivity* (*R*): This rainfall is further used to calculate the rainfall erosivity factor for 2017 and 2024 using an equation given by Singh et al. (1981) [37] for the Indian subcontinent. The equation is

$$R = 79 + 0.363 \times \text{Average Rainfall} \quad (3)$$

- *Soil Erodibility* (*K*): This is a constant defined based on the soil texture classifications on NBSS and LUP maps, with data from the regional literature.
- *Topographic Factor* (*LS*): ALOS-PALSAR DEM at 30 m resolution was procured from the Alaska Satellite Facility (ASF), and mosaicking was carried out. The DEM was converted into ASCII format for the calculation of the LS factor using a tool developed in Arc Macro Language [38] and modified in C++ programming [39]. This methodology ensures the high quality of the data without any gaps or voids and has been previously used in many studies [26,40]. This tool utilized the equation developed by Wischmeier and Smith (1965) [41], which is

$$LS = \left(\frac{l}{72.6}\right)^{m} \left(65.41\sin^2\beta + 4.56\sin\beta + 0.065\right) \quad (4)$$

where l is the cumulative slope length in meters, β is the downhill slope angle, and m is the slope contingent variable.

- *Cover Management Factor* (*C*): Sentinel provides imagery at 10 m spatial resolution, and the derived NDVI using Sentinel imagery shows very high accuracy and spatial distribution of vegetation indices. We calculated the NDVI for both the pre- and post-monsoon periods and then averaged the NDVI values to account for seasonal vegetation fluctuations. The exponential function as proposed by Van der Kniff et al. (2000) [42] was used to calculate the C factor using the NDVI,

allowing for continuous quantification of vegetation cover effects, rather than relying on values from previous literature. The assigned value from the literature may be subject to error, as it is not location-specific, whereas the C factor calculation from the NDVI is site-specific. Pre-monsoon NDVI (March to April) and post-monsoon NDVI (October to November) were used to calculate the annual average NDVI for 2017 and 2024 based on Sentinel-2 images. This average NDVI was used for the calculation of the C factor. Using this NDVI, the C factor was calculated by using the formula given by Van der Kniff et al. (2000) [42] for C factor calculation. The equation is

$$C = \exp\left[-\alpha \frac{\text{NDVI}}{\beta - \text{NDVI}}\right] \quad (5)$$

where α and β are empirical coefficients, the value of α is 2, and the value of β is 1; NDVI is the Normalized Difference Vegetation Index.

- *Support Practice Factor* (*P*): Each LULC class (2017 and 2024) has their values based on published empirical data (e.g., forest = 0.8, farmland = 0.5, built-up = 1). Raster maps were created to show spatial changes in management methods resulting from land use and land cover changes. The final study involved a spatially explicit analysis of the forecasted soil erosion between 2017 and 2024. This change was examined in detail, along with observed land use and land cover changes and shifts in carbon and phosphorus elements, to attribute erosion alterations to specific anthropogenic factors (e.g., the conversion of rangeland to urban land). This method is important because it is more than a simple list of LULC changes. It evaluates the deterioration process by performing statistical correlations between each LULC transition and changes in the C and P elements of the RUSLE framework. This will help identify not only the location of change but also how the changes exacerbate soil erosion. This method can provide practical information regarding the AMS, which is under strong developmental pressure, by determining the most detrimental transitions in land use and modeling the potential impacts of conservation measures. Therefore, it offers a consistent model for assessing land degradation in other stable mountain systems around the world, where preservation of the fragile soil layer is paramount for ecological integrity and sustainable development.

3. Results

3.1. Spatial Temporal Dynamics of Land Use and Land Cover (LULC)

The analysis showed that the Aravalli landscape has undergone significant changes over a two-decade period and yielded contradictory results when moderate-resolution and high-resolution datasets were compared. The MODIS (500 m) product showed a considerable change at the macro level over 20 years (Table 1). The forest cover had grown significantly, increasing by 30.62 km^2 to 264.62 km^2. At the same time, the shrubland area was reduced by 2911.19 km^2, which may indicate either a problem of categorization or the transformation of open natural habitats. The area of cropland increased by 2508 km^2, and urban areas expanded steadily. This means that there is a possibility of land recovery or conversion due to the decrease in the number of barren fields (Figure 2).

Table 1. Different LULC classes of MODIS data and changes in area in sq km (with resolution of 500 m).

Class	2001	2010	2020	Change Detection (2020–2001)	P Factor	C Factor
Forest	30.6164	37.316	264.6212	234.0048	0.8	0.008

Table 1. *Cont.*

Class	2001	2010	2020	Change Detection (2020–2001)	P Factor	C Factor
Shrubland	3907.87	970.791	996.683	−2911.187	0.8	0.1
Permanent Wetlands	3.42189	16.0132	61.8002	58.37831	1	0.001
Croplands	70,719.7	73,611.1	73,227.7	2508	0.5	0.08
Urban and Built-Up	1107.31	1152.48	1256.3	148.99	1	0.1
Barren	192.432	153.947	116.098	−76.334	1	0.45
Waterbodies	8.98976	28.6928	47.1376	38.14784	0	0
Total	75,970.34	75,970.34	75,970.34			

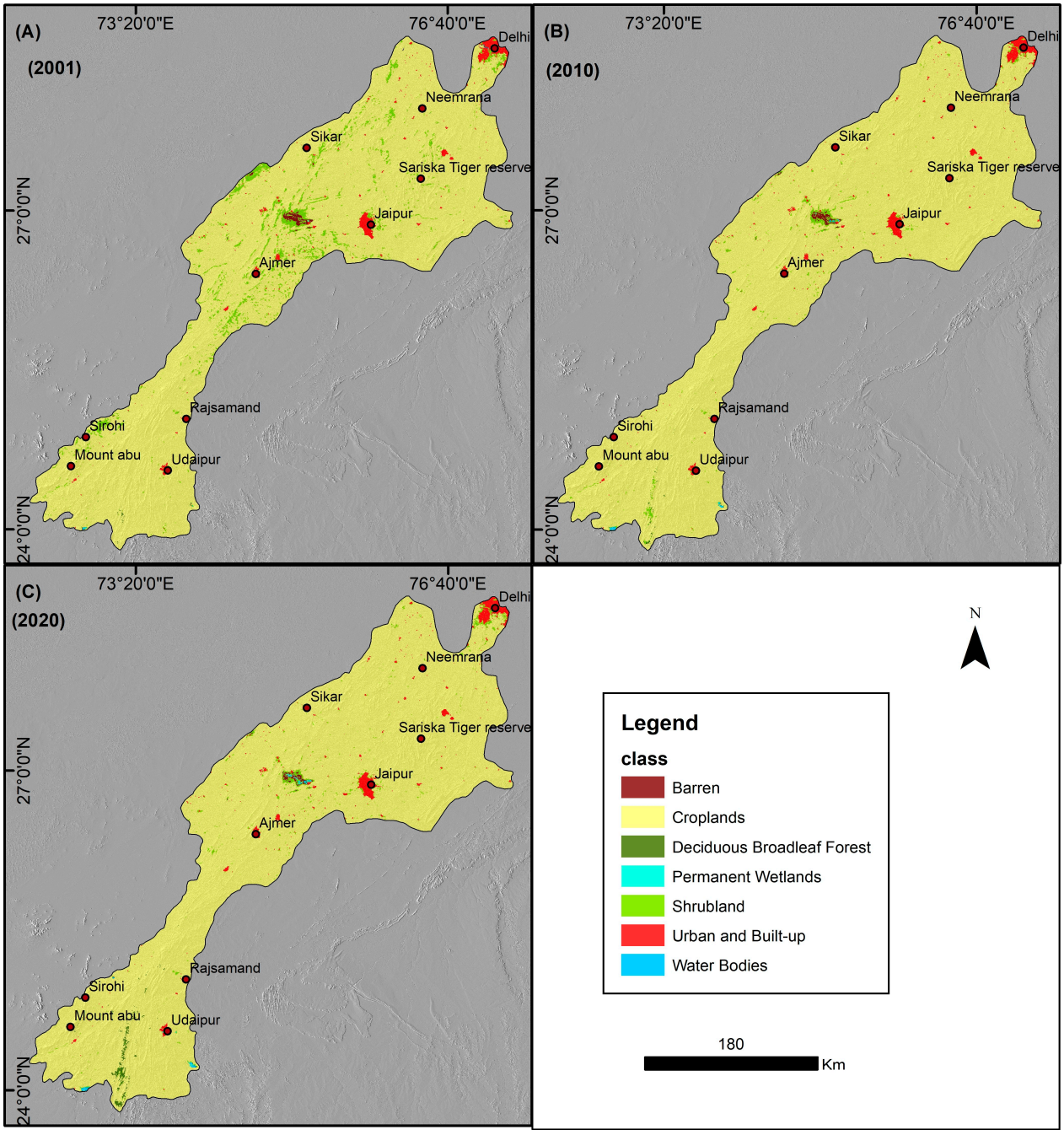

Figure 2. Land use–land cover (LULC) map of the Aravalli region procured from MODIS. (**A**) represents 2001, (**B**) represents 2010, and (**C**) represents 2020. All maps are draped over hillshade.

A more specific description of recent stressors in the ESRI (10 m) analysis is provided (Table 2). The most remarkable change was the accelerated growth of the built-up category by 2644.32 km^2 (53 per cent growth), directly at the expense of natural and semi-natural lands. At the same time, the rangeland (natural grasslands and shrublands) became smaller by 1349.30 km^2, and the cropland would became smaller by 1382.50 km^2, indicating massive land change. Bare land decreased by 101.76 km^2, which could be attributed to the conversion of the land to other uses. There was moderate growth of forest cover by 147.31 km^2 (Figure 3). Such small-scale processes are critical to understanding how degradation works because they directly affect the erosion control variables (C and P). The geographic redistribution of land use and land cover classes altered the intrinsic ability of the landscape to mitigate soil erosion. The average mean P factor (support practice factor) increased from 0.57 in 2017 to 0.64 in 2024, largely due to a shift in land use types that offer less erosion protection, driven by urbanization (Figure 4).

Table 2. Different LULC classes of ESRI data and change in area in sq km, P factor value of each class, and their references (with resolution of 10 m).

S. No.	LULC Class	2017	2024	Change Detection	P Factor	Reference
1	Waterbodies	400.515	440.956	40.44104	0	[43]
2	Forest	1231.85	1379.16	147.31	0.8	[44]
3	Flooded vegetation	5.55089	7.04385	1.49296	0.05	[45]
4	Cropland	44,736.3	43,353.8	−1382.5	0.5	[46]
5	Built-up	4958.84	7603.16	2644.32	1	[46]
6	Bare land	264.784	163.02	−101.764	1	[46]
7	Rangeland	24,372.5	23,023.2	−1349.3	0.8	[47]
	Total	75,970.34	75,970.34			

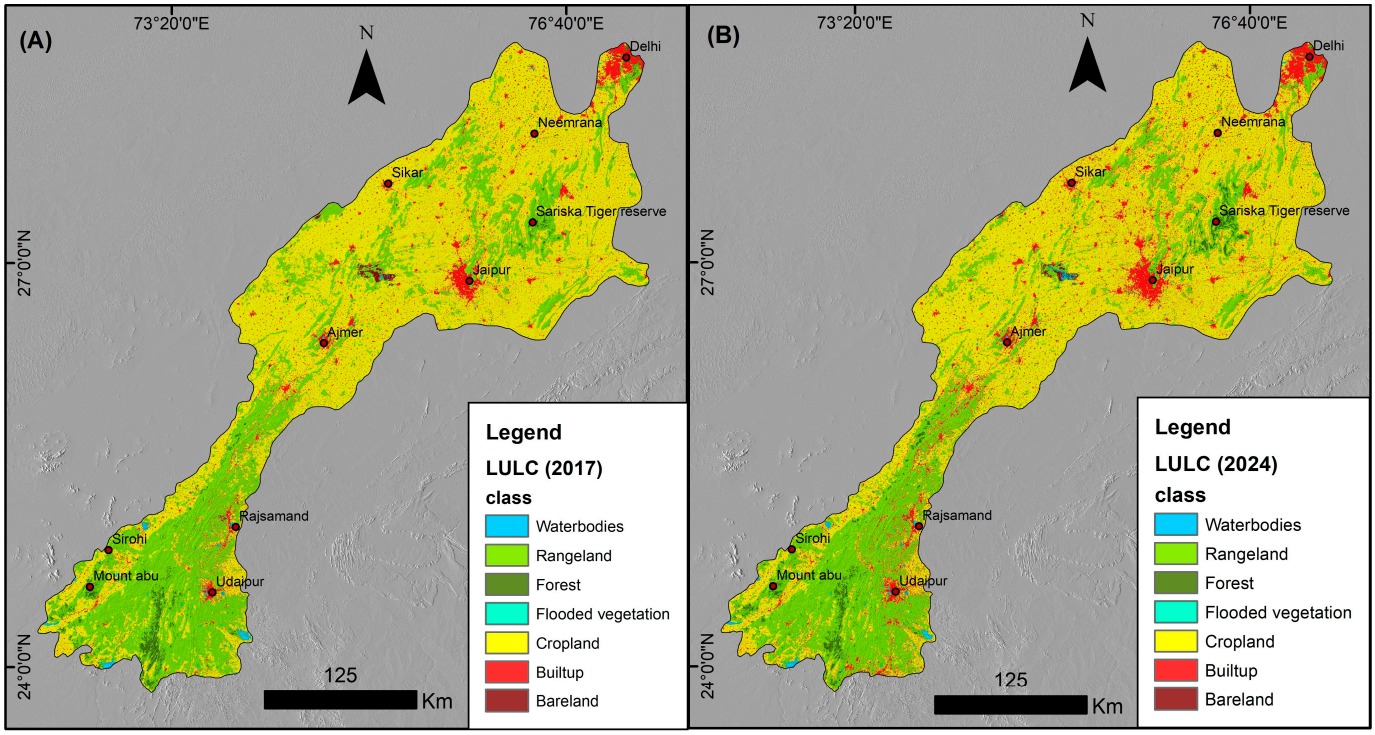

Figure 3. Land use–land cover (LULC) map of the Aravalli region procured from ESRI. (**A**) represents 2017, (**B**) represents 2024. All maps are draped with hillshade.

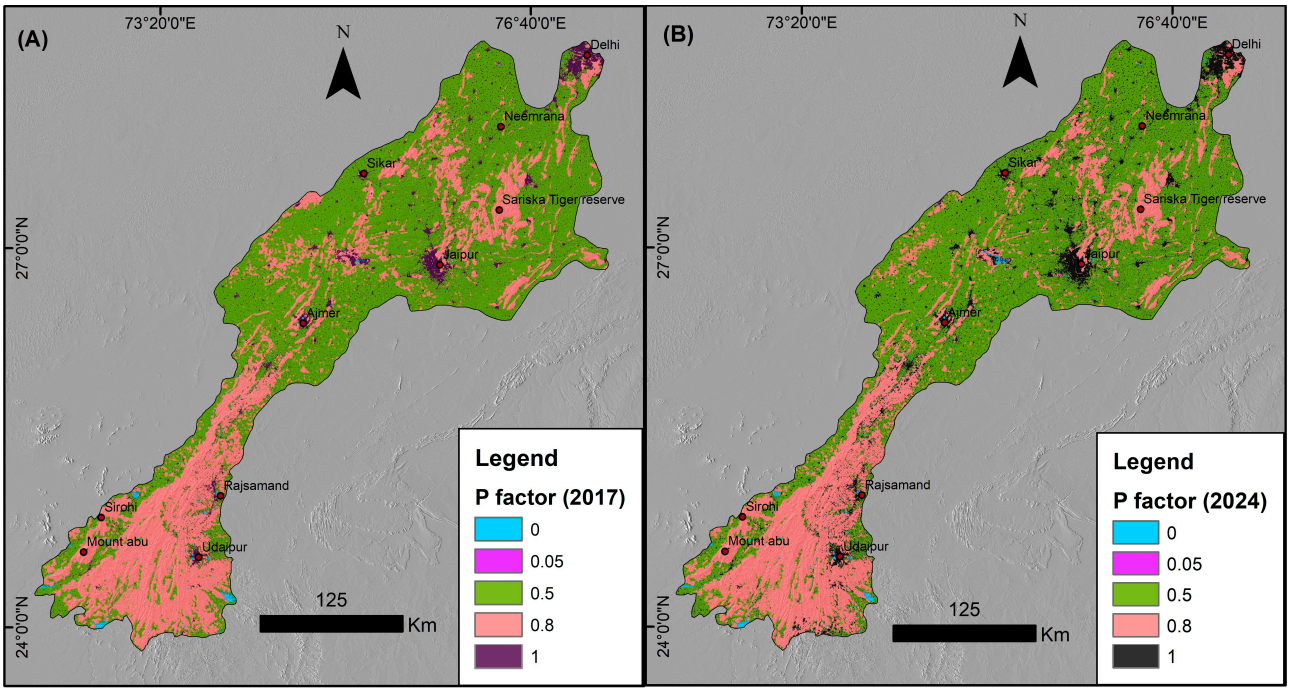

Figure 4. P factor map of the Aravalli region, procured from ESRI LULC. (**A**) represents 2017, (**B**) represents 2024. All maps are draped with hillshade.

3.2. Vegetation Cover (NDVI) and Cover Management Factor (C)

There was a negative trend in vegetation density and health, which are among the main natural barriers to erosion. The average NDVI percentage in the research area dropped to 0.194 in 2024 compared to 0.208 in 2017, indicating a decrease in vegetation vitality (Figure 5). This degradation was accompanied by an increase in the mean C factor (cover management factor), i.e., from 0.58 in 2017 to 0.61 in 2024 (Figure 6), indicating that the ground surface became more susceptible to the effects of raindrops and overland flow.

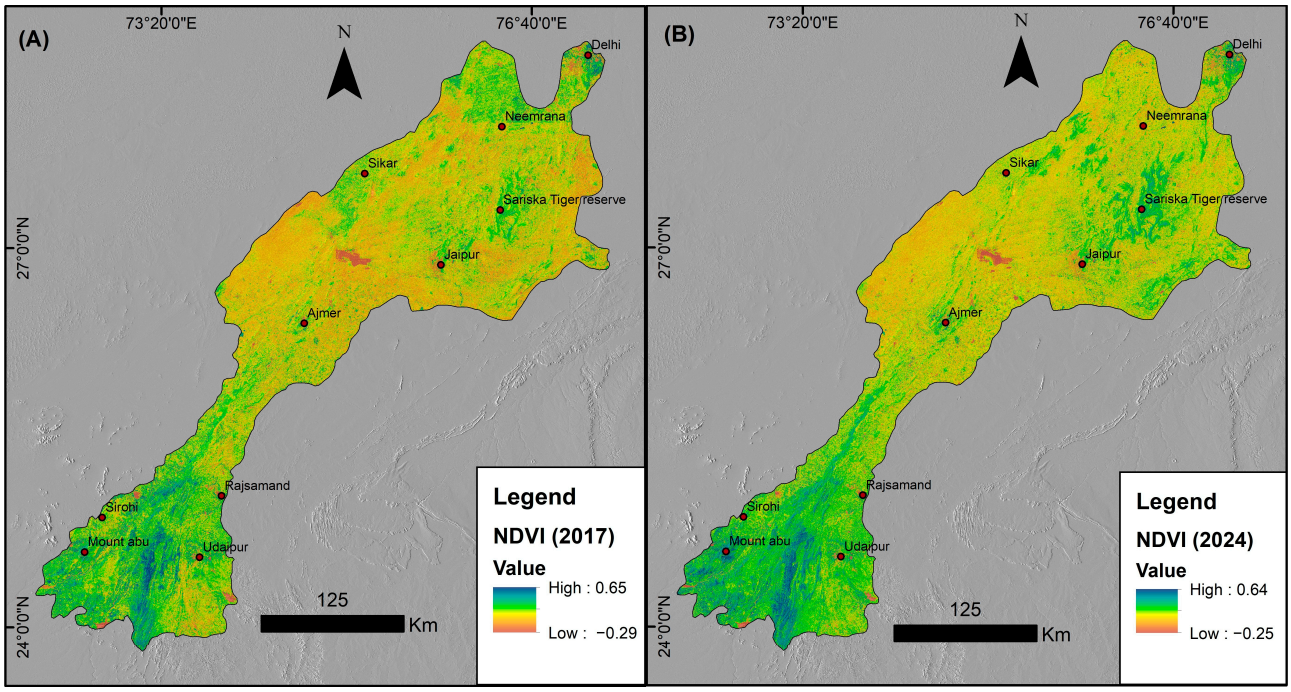

Figure 5. Temporal NDVI of the study area. (**A**) represents the average of the pre–post monsoon of 2017 and (**B**) represents the average of the pre–post monsoon of 2024.

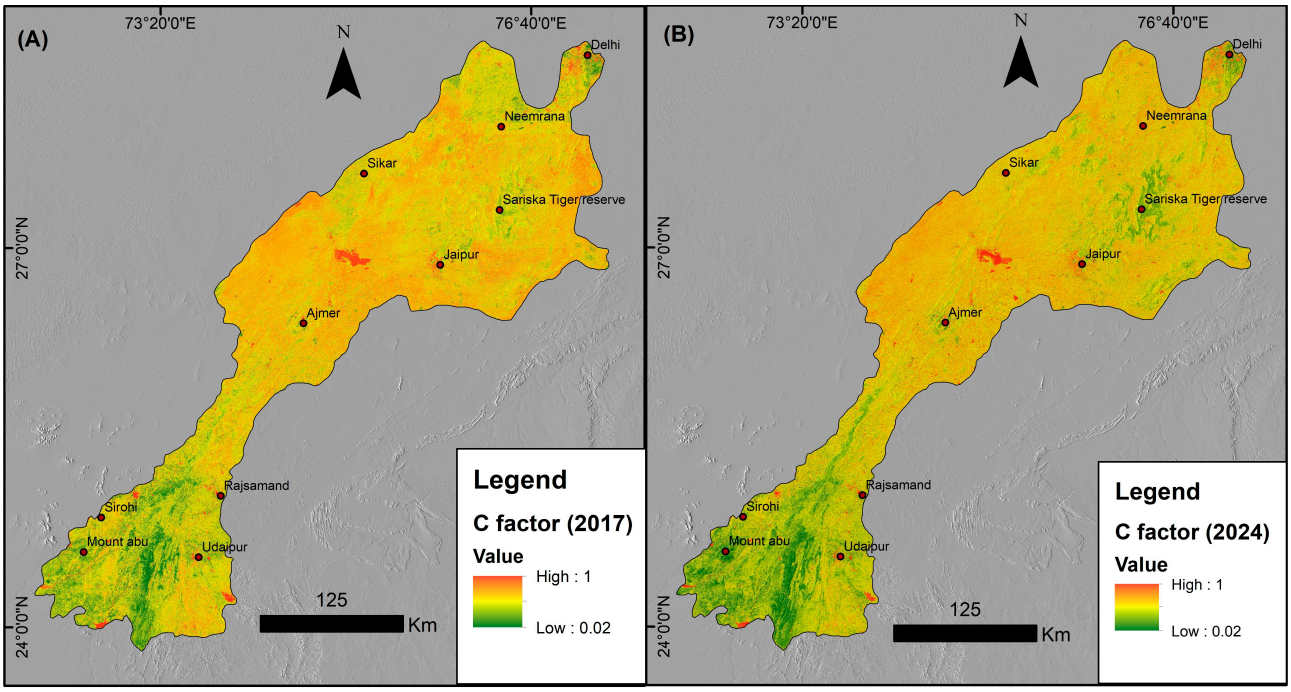

Figure 6. Temporal C factor value of the study area. (**A**) represents the C factor of 2017 and (**B**) represents the C factor of 2024.

3.3. Topographic (LS) and Soil Erodibility (K) Factors

The LS factor, which is the topographic factor influencing erosion derived from the 30 m DEM, had a mean slope steepness (S) of 1.01 and a mean slope length (L) of 0.81, indicating the spatial pattern with the highest steepness slopes and convergent areas (Figure 7). The K factor, a sign of soil intrinsic erodibility, did not change significantly, ranging from 0.011 to 0.118, with a mean of 0.033, which emphasizes that regions of finer, more dispersible soils are, by nature, more susceptible (Figure 8).

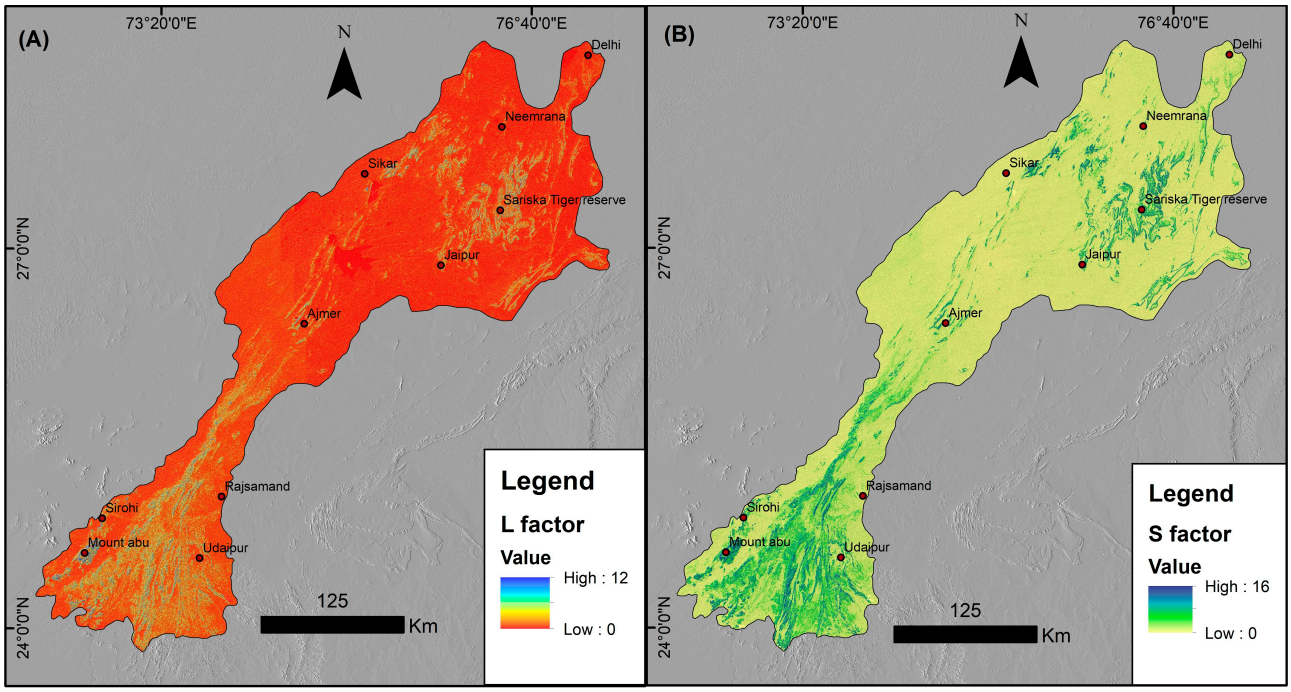

Figure 7. LS factor of the study area calculated using ALOS-PALSAR DEM. (**A**) Slope length (L), (**B**) Slope steepness. All maps are draped with hillshade.

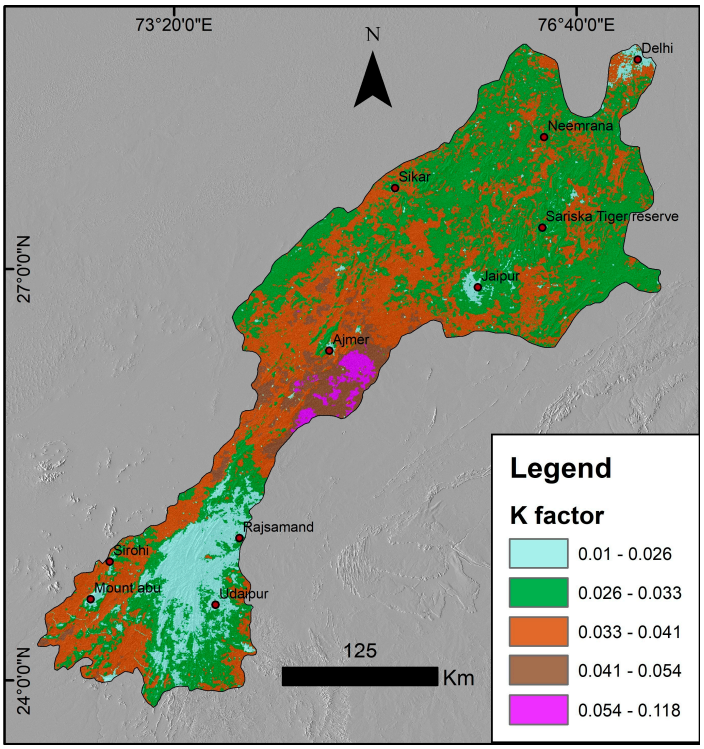

Figure 8. K factor map developed through the K value assigned to each soil texture class.

3.4. Climatic Erosivity (Precipitation and R Factor)

There was considerable geographical variation and inter-annual variation in annual precipitation. The mean rainfall increased from 735.8 mm in 2017 to 1026.2 mm in 2024 (Figure 9). As a result, the rainfall erosivity (R factor) increased by an average of 101.25 MJ mm h^{-1} yr^{-1} to 110.04 in 2024 (Figure 10). An increase of 8.7% in climatic driving force intensified the threat of erosion throughout the region, with the eastern parts of the region that received more precipitation in 2024 being affected more.

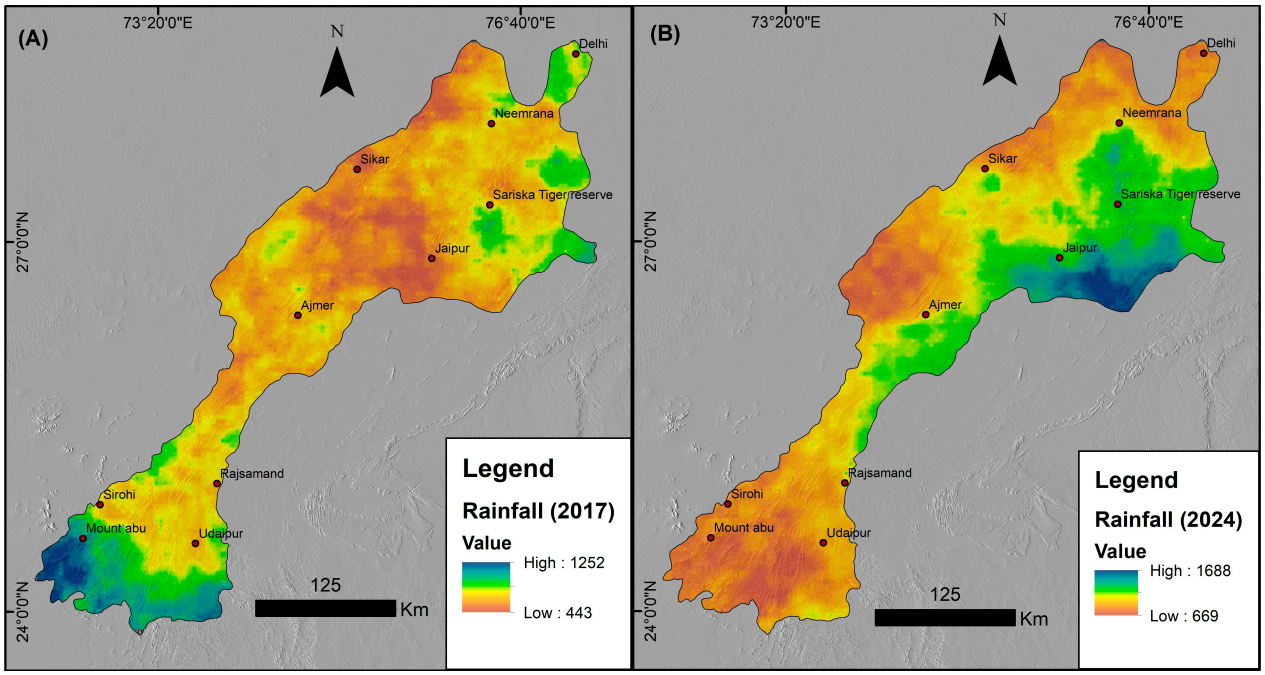

Figure 9. Temporal rainfall data. (**A**) is the rainfall in 2017 in the Aravalli region; (**B**) is the rainfall in 2024.

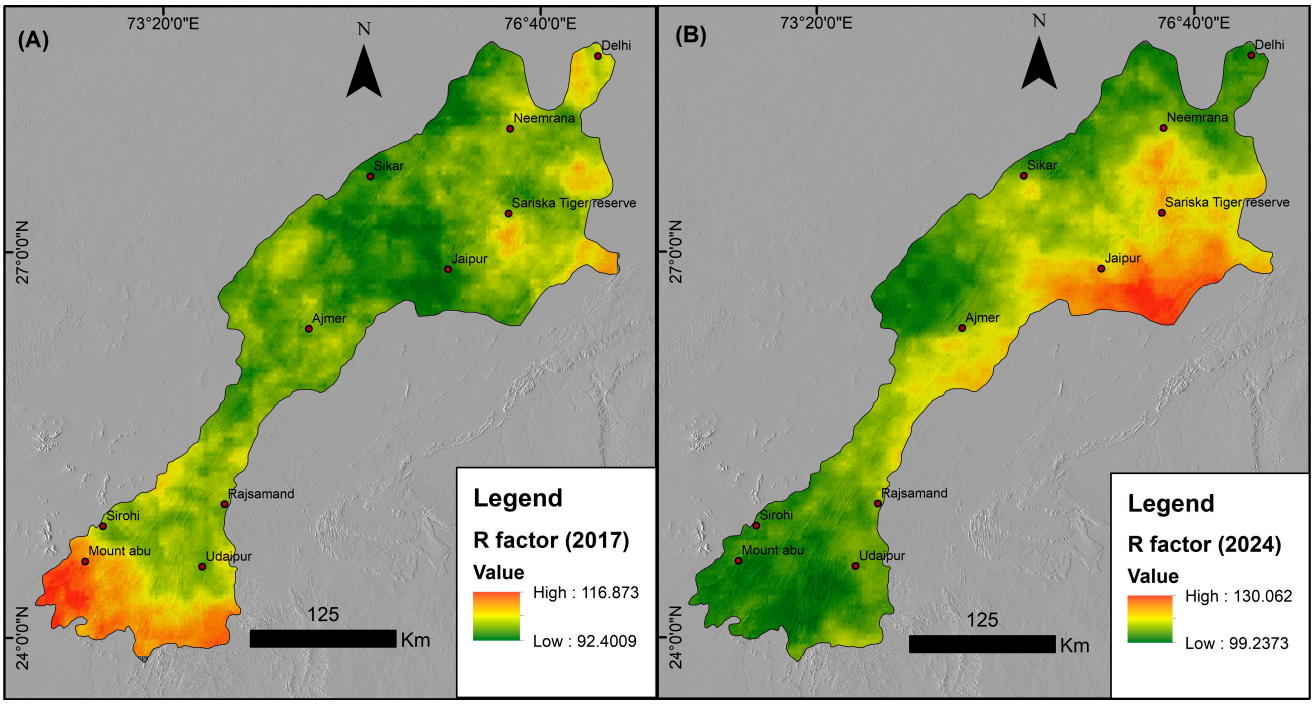

Figure 10. Temporal R factor map of the study area. (**A**) represents 2017, (**B**) represents 2024. All maps are draped over hillshade.

3.5. Soil Erosion Assessment on a Comprehensive Scale

This was achieved by incorporating all dynamic (R, C, P) and static (K, LS) elements into the RUSLE framework to estimate net soil erosion. The estimated average annual soil erosion rate in the Aravalli region increased by 13.8 percentage points between 2017 and 2024 (Figure 11), from 1.59 t/ha/yr^{-1} to 1.81 t/ha/yr^{-1}, respectively. Spatial relationships between the highest erosion rates and steep slopes (high LS), vulnerable soil types (moderate–high K), minimal plant cover (high C) and growing urban or disturbed land (high P) were especially evident in years of high rainfall erosivity (high R). This increase occurred in the face of small increases in forest cover, which highlights that the dominant processes of land conversion, that is, urbanization and rangeland depletion, overrode localized conservation achievements, leading to the net effect of increasing land degradation. To understand the process in detail, we carried out a sensitivity analysis.

A multiple linear regression model was used for both the 2017 and 2024 data (please refer to the Supplementary S2). The results indicate that erosion rates in both years are dominated by topography. The S factor indicates the steepness of the slope; it was 69.8% in 2017 and 69.1% in 2024, indicating that the slope is most sensitive, meaning it accelerates surface runoff and causes higher erosion rates. The other topographic factor, L (slope length), accounts for 17% of the sensitivity to erosion in 2017 and 21.8% in 2024. The R factor shows a 7.2% contribution in 2017 but only 0.3% in 2024, indicating that it is highly sensitive to erosion. Similarly, we compared the MODIV-based soil erosion rates with the sentinel-based soil erosion rates against the underscale-based limitation (see Supplementary S3). To compare erosion rates across different LULC classes, we also calculated erosion rates using MODIS LULC. MODIS LULC was used to calculate the C and P factors using the values assigned to each LULC class. The R factor was calculated using the rainfall of 2000, 2010, and 2020. Only the C, P, and R factors were changed; otherwise, the L, S, and K factors were constant. The results indicate that the erosion rate was 0.17 t/ha/yr in 2001, 0.165 t/ha/yr in 2010, and 0.179 t/ha/yr in 2020 (Supplementary S3). This shows a comparison of LULC

spatial resolutions used to calculate erosion rates; higher spatial resolution captures more features and yields a more accurate spatial distribution of erosion.

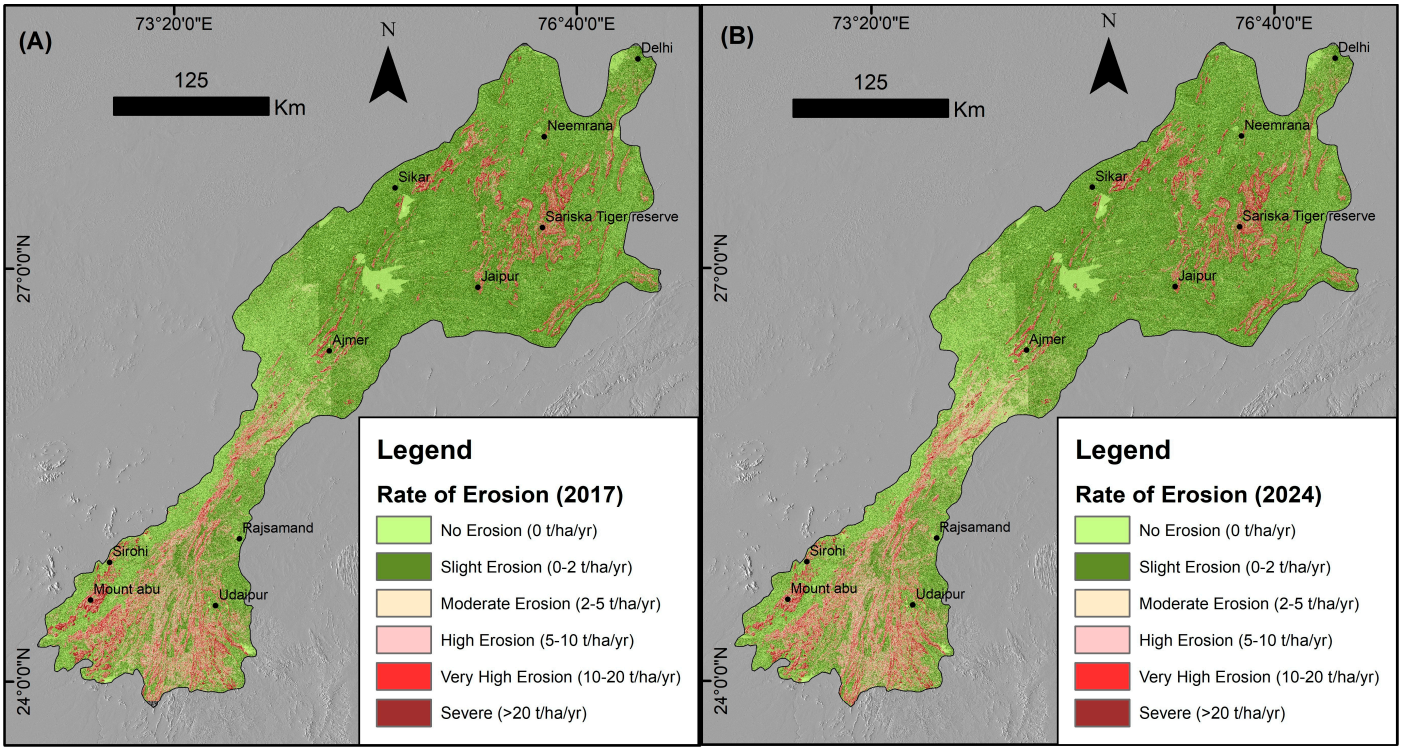

Figure 11. Temporal and spatial distribution of the rate of erosion in the study area. Light green colour indicates no erosion, as the RUSLE model is either not applicable in such conditions, or there is no erosion or very slight erosion in the area. (**A**) represents 2017, (**B**) represents 2024.

3.6. Mining Scenario of the Aravalli Mountain System

Lead–Zinc (Pb-Zn): In the Aravalli province, lead–zinc (±silver) mineralization is one of the most economically viable forms of mining. From 2015 to 2021, lead–zinc mining in Rajasthan occurred under 7–8 active leases covering areas ~6965–7141 ha, with annual production varying between ~30 and 111 Mt. Revenue from lead–zinc (Pb-Zn) mining operations increased over this period, reaching ~INR 254,000 million in 2021, while employment rose from ~6700 workers in 2015 to nearly 30,000 workers by 2021 (Table 3 and Supplementary S1), underscoring the sustained industrial importance of the Aravalli Pb–Zn metallogenic province. This production is dominantly sourced from world-class deposits, such as Rampura–Agucha, Sindesar Khurd, Rajpura–Dariba, and Zawar. Iron Ore: The second most important metallic resource by production volume is iron ore. Its mining from 2015 to 2021 involved 15–18 leases covering areas of ~2230–2345 ha, with annual production ranging between ~25 and 48 Mt. Revenue from iron ore increased steadily, reaching ~INR 10,393 million in 2021, while employment rose from ~830–990 workers (2015–2017) to over 1180 workers in 2021, indicating renewed exploitation of eastern Rajasthan iron ore belts. Copper ore: The mining of copper ore remained spatially restricted in the north and central parts of ARM but economically relevant, with three persistent leases covering ~707 ha throughout the study period. Annual production varied significantly, from ~9.9 Mt in 2020 to ~28.9 Mt in 2021, accompanied by a notable increase in revenue, reaching ~INR 5489 million in 2021. Employment associated with copper mining remained relatively stable at ~1760–1890 workers, consistent with long-established operations in the Khetri Copper Belt. Manganese: Manganese mining represents a smaller but steady component of the metallic resource base, with a single lease covering ~18.9 ha throughout the study

period. Production increased gradually from ~0.03 Mt in 2015 to ~0.13 Mt in 2021, accompanied by modest revenue growth, while employment remained constant at ~70 workers, indicating limited but sustained exploitation of stratiform manganese deposits. Silver: The production of silver occurred primarily as a by-product of Pb–Zn mining. Although no independent silver leases were active, reported silver output increased intermittently, with sale values reaching ~INR 3128 million in 2021, underscoring its economic contribution despite negligible direct employment.

Table 3. Minerals, lease and revenue generated from the mines (metallic) of the Aravalli range (Data source—https://mines.rajasthan.gov.in/dmgcms/page?menuName=Home (Data accessed on 4 January 2026)).

Mineral	Leases	Area	Production	Sale Value	Revenue	Employment	Year
Copper Ore	3	706.75	11.03992	220.7984	1698.28	1890	2015
Iron Ore	17	2235.093	41.3387	795.1189	3084.672	992	2015
Lead–Zinc	8	6964.97	59.00459	1403.909	115,555	6724	2015
Silver	0	0	0.003672	1332.702	6675.44	0	2015
Manganese	1	18.898	0.03457	1.0371	8	70	2015
Copper Ore	3	706.75	10.55287	211.0574	1582.93	1890	2016
Iron Ore	18	2240.099	35.62676	743.8161	3225.276	899	2016
Lead–Zinc	8	6964.97	61.36137	1456.315	158,476.1	7093	2016
Silver	0	0	0.004564	1766.876	12,229.46	0	2016
Manganese	1	18.898	0.02545	0.4072	6.89	70	2016
Copper Ore	3	706.75	11.60267	232.0534	2039.41	1890	2017
Iron Ore	18	2240.097	34.67614	1020.736	1940.418	833	2017
Lead–Zinc	8	7141.27	56.57699	1523.266	185,685.9	7986	2017
Silver	0	0	0.004209	1631.923	11,334.27	0	2017
Manganese	1	18.898	0.07502	2.2506	6.28	70	2017
Copper Ore	3	706.75	13.49566	0	2432.24	1890	2018
Iron Ore	18	2230.099	33.28672	1308.424	2659.635	949	2018
Lead–Zinc	8	6964.973	110.9525	8032.635	208,563.5	28,697	2018
Silver	0	0	0.00158	0	2001	0	2018
Manganese	1	18.898	0.0941	4.705	12.38355	70	2018
Copper Ore	3	706.75	11.49213	0	1851.34	1760	2019
Iron Ore	18	2345.312	25.42375	998.3889	2539.372	957	2019
Lead–Zinc	7	7089.272	0	0	0	26,388	2019
Silver	0	0	0.001351	0	1944.1	0	2019
Manganese	1	18.898	0.09937	2.9811	16.13	70	2019
Copper Ore	3	706.75	9.91991	0	1802.64	1760	2020
Iron Ore	15	2265.645	42.47763	1861.836	5115.946	993	2020
Lead and Zinc	7	7089.273	61.45674	4437.929	183,503.8	27,912	2020
Silver	0	0	0.001204	199.75	22,674.98	0	2020
Manganese	1	18.898	0.0694	2.082	7.6025	70	2020
Copper Ore	3	706.75	28.88911	72.22276	5488.93	1760	2021
Iron Ore	15	2297.065	47.6655	2214.864	10,392.74	1183	2021
Lead and Zinc	7	7089.273	30.44639	5744.762	254,008.2	29,531	2021
Silver	0	0	0.005688	3128.323	23,949.1	0	2021
Manganese	1	18.898	0.130706	4.182579	20.9129	70	2021

In addition to metallic ores, the Aravalli Mountain System hosts a diverse suite of non-metallic and industrial minerals, which collectively dominate mining activity in terms of lease numbers, areal extent, and employment. Between 2015 and 2021, non-metallic mining involved thousands of active leases annually, particularly for building stones, limestone, marble, sandstone, masonry stone, quartz, feldspar, clay minerals, and aggregates. Masonry stone, marble, sandstone, limestone, and granite represent the most extensively exploited commodities. For example, masonry stone mining alone involved

>5600 leases annually, covering ~6405 ha, producing ~840–1293 Mt per year and employing ~52,000–63,000 workers, making it the single largest employer within the mining sector. Marble mining, another hallmark of Rajasthan's mineral economy, was carried out under ~1600–2100 leases, covering ~2823–5273 ha area with annual production of ~80–160 Mt and employment exceeding 20,000–30,000 workers. Industrial minerals such as feldspar, quartz, China clay, ball clay, gypsum, limestone (cement and dimensional grades), dolomite, and rock phosphate also showed consistently high production and revenue figures. Feldspar mining alone involved >1200–1700 leases, covering areas of ~6000–8600 ha, with production commonly exceeding 30–70 Mt per year and employment reaching >10,000 workers by 2021. Aggregates and earth materials (kankar–bajri, brick earth, murram, and gravel) contributed substantially to both production volume and rural employment, particularly during 2015–2017, when land allotment for new mining leases was most pronounced.

4. Discussion and Conclusions

Changes in the AMS landscape: The present study shows that there is an evident growth in overall forest cover at a broad spatial scale (Table 1); its fine-scale measurement shows erosive processes, as well as the sharp growth of built environments (2644.32 km^2) and the subsequent depopulation of the rangelands and croplands (Table 2). The trend is similar to that of other ancient mountain systems worldwide. Integrated LULC-RUSLE studies in the Appalachian Mountains of the eastern United States have demonstrated that the land use legacies of surface mining and ex-urban sprawls have drastically increased sediment yields, impairing aquatic ecosystems hundreds of kilometers downstream [48]. Similar processes are visible in the Aravalli system, where a lack of forest does not afflict the landscapes but through the disintegration and transformation of the larger, stabilizing land matrix [49]. Furthermore, under the conditions of medieval mountain systems (e.g., Sierra Nevada, Spain; Apennines, Italy), where traditional terraced agriculture has been abandoned, new, complex patterns of erosion occur, where changes in land use change C and P factors, providing the latest vulnerability, even after land vegetation growth has recovered [50–52].

The transformation of semi-natural vegetation surfaces to impervious surfaces on the Aravalli has a direct negative effect on the natural defense mechanisms of the land. This loss is statistically shown by an upward change in the mean P factor to 0.64 (poor land management) and an upward change in the C factor to 0.61 (reduced vegetation effectiveness) (Figures 3 and 5). Such a mechanistic inter-relationship between LULC change and the controlling factors of erosion is a strong, recurrent observation worldwide. The steeply inclined expansion of subsistence agriculture, once again observed with the help of the LULC change analysis, has been directly linked to high C factor values and disastrous soil erosion in the highlands of East Africa and the Andes, jeopardizing food security in the region [53–56]. Human-caused erosion of the landscape was accompanied by an 8.7 increase in climatic erosivity (R^2) between 2017 and 2024 (Figure 9). This interdependence of human activity and climate change, in which human activity increases exposure and climate change increases hazards, is characteristic of the contemporary degradation of vulnerable ecosystems across the globe [8]. As a result, a 13.83% increase in mean soil erosion rates (1.59 to 1.81 t/ha/yr) became a direct and foreseeable effect (Figure 10). These results highlight the fact that local conservation benefits, such as afforestation, can be swamped out by large, unsustainable land conversion processes. In a dramatically well-known case, the Loess Plateau in China, initial reforestation was defeated until landscape-scale terracing and sustainable farming (P factor management) were implemented [57–59].

This apparent paradox between increasing forest cover and simultaneously rising erosion rates reflects a broader disconnect between conservation policy targets and landscape-

scale geomorphic responses. The common target of forest conservation, as per "The Forest (Conservation) Act, 1980" and "The Wildlife (Protection) Act, 1972", is conserving forest spaces. Though conservation of forests does imply reduction of soil erosion due to the key ecosystem function [60,61], there are several other reasons for soil erosion. In the case of AMS, the forest cover may have influenced the reduction in soil erosion only when geological variables, such as slope dynamics, precipitation rate, wind velocity, urbanization impact, and mining impact, were kept constant. But, in the case of the AMS, over the years, precipitation is recorded to have been increased [62], wind power is larger in the state of Rajasthan compared to other parts of India [63], and urbanization has increased in the region [64,65], which can affect soil erosion rates despite the temporal increase in forested area. Rather, soil erosion can reduce the resilience of the forest to adapt to environmental stressors [66]. Policies should now incorporate soil erosion dynamics, along with other ecosystem conservation and restoration targets, to achieve a holistic result.

One of the oldest fold systems in the world, the Aravalli Mountains, has experienced land degradation, a complex problem mainly due to land use and land cover (LULC) modification coupled with soil erosion processes. Severely eroded soils and fragile ecosystems of the region maintain a delicate ecological balance, which is especially vulnerable to anthropogenic stress and has become even more intense in recent decades [4]. The major LULC changes, in particular urban growth, mining, deforestation, and agricultural intensification, have had a drastic impact on the natural landscape [67] (Figures 1 and 2). The reduction of the support practice factor (P) as rangelands and croplands are converted to urban areas and the worsening of the cover management factor (C), as evidenced by a decrease in NDVI values between 2017 and 2024, have deteriorated (Figure 5). These changes increase the vulnerability of soils to erosive power, especially at a time when rainfall erosivity (R factor) has increased by 8.7 per cent (Figure 9). Similar land degradation patterns have been observed in other ancient mountain systems, such as the Appalachians (North America), the Mediterranean highlands (Europe), and the Andes (South America) [68–70]. In the long term, anthropogenic processes across all of these regions, especially land cover transformation and unsustainable land management, have led to increased soil erosion and ecosystem degradation. An example is the Mediterranean highlands, where soil loss after deforestation is severe and agricultural activities have been deserted, and urban sprawl and mining in the Appalachian terrain, where natural processes of soil retention have been disrupted [69]. These case studies support the finding that the interaction between LULC dynamics and soil erosion is a key driver of land degradation in both old mountain systems.

Policy, Governance, and Mining: The Supreme Court of India, in its ruling on 20 November 2025, redefined the Aravalli Hills and Aravalli Ranges based on the altitude. The judgment delivered in RE: ISSUE RELATING TO DEFINITION OF ARAVALI HILLS AND RANGES concerns the legal definition and conservation of the Aravalli Mountain System (AMS). In its judgment, the Court characterized the AMS as one of the oldest geological features, noting that it "is one of the oldest fold mountains in India" and that scientific assessments establish the Aravalli ecosystem as a "green barrier" preventing desertification, thereby influencing the climate and biodiversity across northern India. As part of its directions, the Court directed that no fresh mining leases or renewals of existing mining leases should be permitted in the Aravalli Hills and Ranges, as defined in the Forest Survey of India (FSI) report dated 25 August 2010, without permission from the Supreme Court. Subsequently, in a follow-up order issued on 29 December 2025, the Supreme Court acknowledged the presence of ambiguities in the implementation of the 20 November 2025 judgment. It directed the constitution of a high-powered expert committee to re-examine the adopted definition and its ecological and regulatory implications. The Court also

stayed the implementation of specific operative directions of the original judgment pending further expert review. This ruling came after widespread popular protests and concerns about the risks posed by unregulated mining in the ecologically sensitive Aravalli landscape. To also avoid the amended definition being used to validate unchecked extraction efforts and to create a more coherent structure for how the environment will be preserved. The case will be brought back for another hearing on 21 January 2026, during which the existing ambiguities and questions regarding the use of the new definition will be resolved. This shows how these judicial developments establish an evolving policy and governance framework that is expected to shape future land use regulation and conservation planning in the AMS, thereby forming an essential contextual driver of contemporary and future LULC transitions in the region.

Mining activity provides an additional and quantifiable driver of land transformation in the Aravalli Mountain System. Rajasthan contains approximately 550–600 km of the total ~800 km length of the AMS, and mining statistics from 2015 to 2021 (Department of Mines and Geology, Rajasthan, India) indicate strong decoupling between the areal footprint and economic returns in the Aravalli Mountain System, with significant consequences for landscape modification. Metallic minerals, especially lead and zinc, generated remarkably high and rapidly escalating revenues from a comparatively confined and stable lease area (approximately 7000 ha), indicating progressive intensification through deeper mining, higher-grade extraction, and enhanced beneficiation rather than lateral expansion. This trend markedly differs from that of non-metallic and industrial minerals, whose income growth is intricately linked to enormous spatial development, as evidenced by numerous leases and significant land use for masonry stone, marble, sandstone, limestone, and aggregates. Despite lower unit earnings from these commodities, their economic impact is substantial due to high volume and employment intensity; unfortunately, this has resulted in extensive surface disruption, increased quarrying, and fragmentation of the Aravalli landscape. The period from 2015 to 2017, characterized by rapid lease distribution and area growth, marks a phase of intensified physical alteration of the mountain range. In contrast, trends since 2018 suggest a focus on income optimization within an already expanded spatial footprint. These patterns indicate that metallic mining consolidates economic value with relatively limited land disturbance, whereas non-metallic mining significantly alters the geomorphology and ecology of the Aravalli landscape. This underscores the necessity to incorporate real impact per unit revenue into future mineral governance and land use planning in this ecologically sensitive orogen. The scale, spatial distribution, and intensity of mineral exploitation outlined above provide an essential context for assessing the environmental sensitivity and landscape response of the Aravalli Mountain System.

LULC changes and soil erosion are vital to understanding land degradation for several reasons. First, they allow for quantifying degradation processes rather than relying on qualitative observations and conducting targeted interventions [71]. Using RUSLE in the present study, it is possible to identify spatial erosion hotspots by incorporating climatic, topographic, and edaphic factors, along with anthropogenic factors, into a comprehensive evaluation of degradation risk [72]. Second, it links land cover changes to particular erosion control properties (C and P), without which it is impossible to design efficient conservation and land management strategies, especially when development stressors threaten ecological quality and sustainable development, such as in Aravalli [3]. Additionally, the capability to predict soil erosion patterns against the projected land use conditions will enable policymakers and land managers to have proactive information to avert the soil erosion process before irreparable damage occurs [73]. The subsequent acceleration in the rate of soil erosion observed despite moderate improvements in the forest cover reflects the overwhelming effect of urbanization and degradation of the rangelands, and, therefore,

there is a need to have integrated land use planning that incorporates both development and conservation goals [74–76]. As per national reports, there has been a recorded increase in overall forest cover across India by 156.41 km^2, as per INDIA STATE OF FOREST REPORT 2023, indicating a successful forest conservation strategy by the government of India [https://www.fsi.nic.in/forest-report-2023 (accessed on 26 February 2026)].

The present study suggests that the Aravalli Mountain System, one of the planet's oldest fold mountains, is experiencing an extreme and rapid process of land degradation, in tandem with a global trend toward degraded and old scenery. The leading cause is the systematic transformation of stabilizing vegetated lands, rangelands, and croplands into urban and built-up surfaces, which directly reduces the C and P factors that govern erosion [77,78]. Adding this to observable increases in rainfall erosivity (R factor) has resulted in an average increase in soil loss of 13.8 per cent from 2017 to 2024. The implications, backed by global examples, such as the Appalachians to the Andes, are apparent: the weakness of old mountains is their weak balance, which is imbalanced by anthropogenic land cover change [79,80]. To ensure the protection of these landscapes, it is necessary to go beyond individual afforestation projects and implement a strategic, spatially explicit land use planning approach that focuses on preserving the entire natural and semi-natural vegetation matrix to achieve low C and P factors [81–83]. The conceptualization of degradation based on the combined perspectives of LULC change and process-based soil erosion modeling is therefore an operational requirement [84]. This strategy, tested across continents, provides empirical evidence to support the idea of sustainable development, implement strict conservation strategies, and create pro-cyclical erosion control plans. In this way, we will be able to take steps to protect the precious ecological services, such as water security, biodiversity, and climate management, that these ancient mountains can offer future generations.

The terrestrial degradation experienced in the Aravalli Mountain System over the last 20 years is largely driven by high land use and land cover change and enhanced soil erosion influenced by climatic and topographic conditions. Being one of the oldest mountain systems, the weak soil and ecosystems of Aravalli are highly exposed to anthropogenic disruptions, especially in cases of urban growth and land use conversion, which have increased the threat of erosion and the vulnerability of the ecosystems. The quantification of the land degradation process, the identification of key areas of focus, and the creation of specific conservation policies are only possible by studying land degradation through LULC transformations and soil erosion models, such as RUSLE [71,84]. The combination of high-resolution spatial information with erosion modeling provides a robust framework for understanding and controlling land degradation in a delicate mountain setting [55,85,86]. To effectively manage the Aravalli Mountains, the factors driving land change in the area must be addressed by implementing sustainable land use measures to minimize erosion and maintain a healthy ecological state. The study helps us gain pertinent information on the spatial–temporal dynamics of land degradation. It presents a common approach that can be used in other stable mountain systems with the same problems elsewhere in the world.

Supplementary Materials: The following supporting information can be downloaded at https://www.mdpi.com/article/10.3390/geographies6010029/s1, Supplementary S1: Minerals, leases, and revenue generated from the mines (other materials) of the Aravalli range; Supplementary S2: Sensitivity analysis; Supplementary S3: Predicted soil erosion comparison; Supplementary S4: Dataset sources.

Author Contributions: Conceptualization, R.D. and A.C.; methodology, R.K. and RD.; software, R.K. and R.D.; validation, R.D. and J.K.R.; formal analysis, R.K. and R.D.; investigation, J.K.R. and

R.D.; resources, R.K. and R.D.; data curation, R.D. and R.K.; writing—original draft preparation, R.D., R.K., J.K.R., and A.C.; writing—review and editing, R.D., A.C., and J.K.R.; visualization, R.D. and R.K.; supervision R.D. and A.C. All authors have read and agreed to the published version of the manuscript.

Funding: This research received no external funding.

Institutional Review Board Statement: Not applicable.

Informed Consent Statement: Not applicable.

Data Availability Statement: The data for this study was derived from MODIS (https://modis.gsfc.nasa.gov/data/dataprod/mod12.php15]), ESRI (https://livingatlas.arcgis.com/landcoverexplorer/#mapCenter=-3.28600,31.34000,3.00&mode=step&timeExtent=2017,2021&year=2022&downloadMode=true), NBSS and LUP (https://icar-nbsslup.org.in/), Alaska Satellite facility (https://search.asf.alaska.edu/), and CHRS (https://chrsdata.eng.uci.edu/). Data accessed on 4 January 2026.

Acknowledgments: R.D., R.K., and A.C. acknowledge O.P. Jindal Global University for providing the infrastructure to conduct this study. J.Y. acknowledges the Indian Institute of Technology Kharagpur for providing infrastructure. The authors have reviewed and edited the output and take full responsibility for the content of this publication. We used Grammarly for editing.

Conflicts of Interest: The authors have no conflicts of interest.

Abbreviations

The following abbreviations are used in this manuscript:

LULC	Land use–land cover
RUSLE	Revised Universal Soil Loss Equation Model
AMS	Aravalli Mountain System

References

1. Nkonya, E.; Mirzabaev, A.; Von Braun, J. *Economics of Land Degradation and Improvement—A Global Assessment for Sustainable Development*; Springer Nature: Berlin/Heidelberg, Germany, 2016.
2. Egholm, D.L.; Knudsen, M.F.; Sandiford, M. Lifespan of Mountain Ranges Scaled by Feedbacks between Landsliding and Erosion by Rivers. *Nature* **2013**, *498*, 475–478. [CrossRef] [PubMed]
3. Hu, X.; Næss, J.S.; Iordan, C.M.; Huang, B.; Zhao, W.; Cherubini, F. Recent Global Land Cover Dynamics and Implications for Soil Erosion and Carbon Losses from Deforestation. *Anthropocene* **2021**, *34*, 100291. [CrossRef]
4. Nampak, H.; Pradhan, B.; Mojaddadi Rizeei, H.; Park, H. Assessment of land cover and land use change impact on soil loss in a tropical catchment by using multitemporal SPOT-5 satellite images and Revised Universal Soil Loss Equation model. *Land Degrad. Dev.* **2018**, *29*, 3440–3455. [CrossRef]
5. Talukder, B.; Ganguli, N.; Matthew, R.; vanLoon, G.W.; Hipel, K.W.; Orbinski, J. Climate change-triggered Land Degradation and Planetary Health: A Review. *Land Degrad. Dev.* **2021**, *32*, 4509–4522. [CrossRef]
6. Istanbulluoglu, E.; Bras, R.L. Vegetation-modulated Landscape Evolution: Effects of Vegetation on Landscape Processes, Drainage Density, and Topography. *J. Geophys. Res.* **2005**, *110*, 2004JF000249. [CrossRef]
7. Kumar, R.; Naqvi, H.R.; Devrani, R.; Deshmukh, B.; Huang, J.-C. Sediment Yield Assessment, Prioritization and Control Practices in Chambal River Basin Employing SYI Model. *J. Geol. Soc. India* **2022**, *98*, 1585–1594. [CrossRef]
8. Guerra, C.A.; Rosa, I.M.D.; Valentini, E.; Wolf, F.; Filipponi, F.; Karger, D.N.; Nguyen Xuan, A.; Mathieu, J.; Lavelle, P.; Eisenhauer, N. Global Vulnerability of Soil Ecosystems to Erosion. *Landsc. Ecol.* **2020**, *35*, 823–842. [CrossRef]
9. Wang, J.; Edwards, P.J.; Hamons, G.W.; Goff, W.A. Assessing RUSLE and Hill-Slope Soil Movement Modeling in the Central Appalachians. In *Proceedings of the 2010 Pittsburgh, PA, USA, 20–23 June 2010*; American Society of Agricultural and Biological Engineers: St. Joseph, MI, USA, 2010; p. 1.
10. Srivastava, A.; Kinnaird, T.; Sevara, C.; Holcomb, J.A.; Turner, S. Dating Agricultural Terraces in the Mediterranean Using Luminescence: Recent Progress and Challenges. *Land* **2023**, *12*, 716. [CrossRef]
11. Hollis, C.J.; Taylor, K.W.; Handley, L.; Pancost, R.D.; Huber, M.; Creech, J.B.; Hines, B.R.; Crouch, E.M.; Morgans, H.E.; Crampton, J.S. Early Paleogene Temperature History of the Southwest Pacific Ocean: Reconciling Proxies and Models. *Earth Planet. Sci. Lett.* **2012**, *349*, 53–66. [CrossRef]

12. Lakkad, A.P.; Patel, D.P.; Nayak, D.; Shrivastava, P.K. Preparation of Erosion Susceptibility Map of Dhaman Khadi Sub-Watershed in Eastern Gujarat Using ArcGIS Interface. *J. Appl. Nat. Sci.* **2016**, *8*, 2196–2202. [CrossRef]
13. Machiwal, D.; Katara, P.; Mittal, H. Estimation of Soil Erosion and Identification of Critical Areas for Soil Conservation Measures Using RS and GIS-Based Universal Soil Loss Equation. *Agric. Res.* **2015**, *4*, 183–195. [CrossRef]
14. Jodhani, K.H.; Patel, D.; Madhavan, N.; Singh, S.K. Soil Erosion Assessment by RUSLE, Google Earth Engine, and Geospatial Techniques over Rel River Watershed, Gujarat, India. *Water Conserv. Sci. Eng.* **2023**, *8*, 49. [CrossRef]
15. Dasgupta, A.; Sastry, K.L.N.; Dhinwa, P.S.; Rathore, V.S.; Nathawat, M.S. Identifying Desertification Risk Areas Using Fuzzy Membership and Geospatial Technique—A Case Study, Kota District, Rajasthan. *J. Earth Syst. Sci.* **2013**, *122*, 1107–1124. [CrossRef]
16. Yadav, B.K.; Malav, L.C.; Ballesta, R.J.; Kumawat, C.; Patra, A.; Patel, A.; Jangir, A.; Nogiya, M.; Meena, R.L.; Moharana, P.C.; et al. Modeling and Assessment of Land Degradation Vulnerability in Arid Ecosystem of Rajasthan Using Analytical Hierarchy Process and Geospatial Techniques. *Land* **2022**, *12*, 106. [CrossRef]
17. Raj, A.; Sharma, L.K. Assessment of Land-Use Dynamics of the Aravalli Range (India) Using Integrated Geospatial and CART Approach. *Earth Sci. Inform.* **2022**, *15*, 497–522. [CrossRef]
18. Paul, N.C.; Reddy, G.P.O.; Kumar, N.; Reddy, K.S.; Gaikwad, B.B.; Nangare, D.D.; Patil, N.G.; Mohekar, D.S. Mapping and Assessment of Abiotic Stresses in Hot Semi-Arid Ecosystem of Western India Using Analytical Hierarchy Process and Machine Learning Models. *Environ. Earth Sci.* **2025**, *84*, 276. [CrossRef]
19. Mukherjee, D.; Rajvanshi, A. Application of Strategic Environmental Assessment as a Land Use Planning Tool in India: A Case of Gurgaon-Manesar Development Plan, Haryana, India. *J. Environ. Assess. Policy Manag.* **2016**, *18*, 1650017. [CrossRef]
20. Mehra, M.; Singh, C.K. Spatial Analysis of Soil Resources in the Mewat District in the Semiarid Regions of Haryana, India. *Environ. Dev. Sustain.* **2018**, *20*, 661–680. [CrossRef]
21. Subramanyan, A.; Dharmaraj, R.; Gurumurthy, K.T.; Sampangi, S.; Srinivasaiah, Y.K.H. Assessment of Land Degradation Due to Soil Erosion Based on Current Land Use/Landcover Pattern Using RS and GIS Techniques. *Arab. J. Geosci.* **2023**, *16*, 431. [CrossRef]
22. Kumar, A.; Golani, P.R. Unique Geosites around Zawar, Rajasthan, Western India: Its Linkage with Ancient Mining-Metallurgy and Archaeological Geodiversity. *Geoheritage* **2023**, *15*, 80. [CrossRef]
23. Kumar, R.; Kasana, P.; Devrani, R.; Devrani, S.P. The Chambal Badlands of Ganga River Basin, India: A Fading Geoheritage Odyssey. *Geoheritage* **2024**, *16*, 93. [CrossRef]
24. Malav, L.C.; Yadav, B.K.; Tailor, B.L.; Pattanayak, S.; Singh, S.V.; Kumar, N.; Reddy, G.P.O.; Mina, B.L.; Dwivedi, B.S.; Jha, P.K. Mapping of Land Degradation Vulnerability in the Semi-Arid Watershed of Rajasthan, India. *Sustainability* **2022**, *14*, 10198. [CrossRef]
25. Kumar, R.; Devrani, R.; Pandey, M.; Deshmukh, B.; Costache, R. Semi-Automated Pixel and OBIA Based Approaches for Gully Feature Extraction in the Lower Chambal River Basin, Central India. *Int. J. River Basin Manag.* **2025**, 1–23. [CrossRef]
26. Kumar, R.; Deshmukh, B.; Kumar, A. Using Google Earth Engine and GIS for Basin Scale Soil Erosion Risk Assessment: A Case Study of Chambal River Basin, Central India. *Proc. Indian Acad. Sci. Earth Planet. Sci.* **2022**, *131*, 228. [CrossRef]
27. Borrelli, P.; Robinson, D.A.; Fleischer, L.R.; Lugato, E.; Ballabio, C.; Alewell, C.; Meusburger, K.; Modugno, S.; Schütt, B.; Ferro, V. An Assessment of the Global Impact of 21st Century Land Use Change on Soil Erosion. *Nat. Commun.* **2017**, *8*, 2013. [CrossRef]
28. Dixit, Y.; Hodell, D.A.; Giesche, A.; Tandon, S.K.; Gázquez, F.; Saini, H.S.; Skinner, L.C.; Mujtaba, S.A.; Pawar, V.; Singh, R.N. Intensified Summer Monsoon and the Urbanization of Indus Civilization in Northwest India. *Sci. Rep.* **2018**, *8*, 4225. [CrossRef]
29. Raj, A.; Sharma, L.K. Eco-Biophysical Indicators to Ascertain the Sustainability Aspect of World's Primitive Hills Range Using Time-Series MODIS Data Products. *Ecol. Inform.* **2022**, *69*, 101650. [CrossRef]
30. Ganguly, T.; Arya, D.S.; Paul, P.K. Spatio-Temporal Patterns of Precipitation in Arid and Semi-Arid Regions in Western India. *J. Earth Syst. Sci.* **2023**, *132*, 71. [CrossRef]
31. Pippal, P.; Kumar, R.; Singh, A.; Rajamani, P.; Kushwaha, A.; Surela, N.; Kumar, R. Chemical Characterization of Trace Elements in PM2. 5 and PM10 and Their Source Apportionment by PMF Modelling with Associated Health Risk Assessment in the Aravalli Region, India. *Res. Sq.* 2025, *ahead of print*. [CrossRef]
32. Sharma, L.K.; Raj, A.; Sharma, S. *The Aravalli Range's Past, Present and Future Prospects: India's Natural Green Wall*; Cambridge Scholars Publishing: Newcastle upon Tyne, UK, 2025.
33. Kaul, V. How a Court Definition Could Weaken Protection of the Aravallis. Available online: https://frontline.thehindu.com/environment/aravalli-supreme-court-mining-groundwater-protests-environment-ecology/article70439452.ece (accessed on 26 February 2026).
34. Aravalli Redefinition Row Explained: Supreme Court Order, Protests and Government's Stand | India News—Times Now. Available online: https://www.timesnownews.com/india/aravalli-redefinition-row-explained-supreme-court-order-protests-and-governments-stand-article-153365635 (accessed on 13 January 2026).

35. Dutta, D.; Rahman, A.; Paul, S.K.; Kundu, A. Changing Pattern of Urban Landscape and Its Effect on Land Surface Temperature in and around Delhi. *Environ. Monit. Assess.* **2019**, *191*, 551. [CrossRef]
36. Sidle, R.C.; Jarihani, B.; Kaka, S.I.; Koci, J.; Al-Shaibani, A. Hydrogeomorphic Processes Affecting Dryland Gully Erosion: Implications for Modelling. *Prog. Phys. Geogr. Earth Environ.* **2019**, *43*, 46–64. [CrossRef]
37. Singh, G.; Chandra, S.; Babu, R. *Soil Loss and Prediction Research in India*; Bulletin No T-12 D; Central Soil and Water Conservation Research Training Institute: Dehradun, India, 1981; Volume 9.
38. Hickey, R. Slope Angle and Slope Length Solutions for GIS. *Cartography* **2000**, *29*, 1–8. [CrossRef]
39. Van Remortel, R.; Maichle, R.; Hickey, R. Computing the RUSLE LS Factor Based on Array-Based Slope Length Processing of Digital Elevation Data Using a C++ Executable. *Comput. Geosci.* **2004**, *30*, 1043–1053. [CrossRef]
40. Kumar, R.; Khaira, J.K.; Ahmed, R.; Devrani, R.; Deshmukh, B. Land Degradation Vulnerability Mapping Using Geospatial Techniques: A Case Study of Nandakini River Basin, NW Himalaya, India. *Int. J. River Basin Manag.* **2024**, *24*, 161–176. [CrossRef]
41. Wischmeier, W.H.; Smith, D.D. *Predicting Rainfall-Erosion Losses from Cropland East of the Rocky Mountains: Guide for Selection of Practices for Soil and Water Conservation*; Agricultural Research Service, US Department of Agriculture: Washington, DC, USA, 1965.
42. Van der Knijff, J.M.; Jones, R.J.A.; Montanarella, L. *Soil Erosion Risk Assessment in Europe*; European Commission: Brussels, Belgium, 2000.
43. Jain, S.K.; Kumar, S.; Varghese, J. Estimation of soil erosion for a Himalayan watershed using GIS technique. *Water Resour. Manag.* **2001**, *15*, 41–54. [CrossRef]
44. Pandey, A.; Chowdary, V.M.; Mal, B.C. Identification of critical erosion prone areas in the small agricultural watershed using USLE, GIS and remote sensing. *Water Resour. Manag.* **2007**, *21*, 729–746. [CrossRef]
45. Brema, J.; Hauzinger, J. Estimation of the soil erosion in cauvery watershed (Tamil Nadu and Karnataka) using USLE. *IOSR J. Environ. Sci. Toxicol. Food Technol.* **2016**, *10*, 1–11.
46. Wanielista, M.P.; Yousef, Y.A. *Stormwater Management*; John Wiley & Sons: Hoboken, NJ, USA, 1992.
47. Jain, M.K.; Mishra, S.K.; Shah, R.B. Estimation of sediment yield and areas vulnerable to soil erosion and deposition in a Himalayan watershed using GIS. *Curr. Sci.* **2010**, *98*, 213–221.
48. Wang, Y.; Zhao, J.; Zhou, Y.; Zhang, H. Variation and Trends of Landscape Dynamics, Land Surface Phenology and Net Primary Production of the Appalachian Mountains. *J. Appl. Remote Sens.* **2012**, *6*, 061708. [CrossRef]
49. Bhattacharyya, R.; Bhatia, A.; Ghosh, B.N.; Santra, P.; Mandal, D.; Kumar, G.; Singh, R.J.; Madhu, M.; Ghosh, A.; Mandal, A.K.; et al. Soil Degradation and Mitigation in Agricultural Lands in the Indian Anthropocene. *Eur. J. Soil Sci.* **2023**, *74*, e13388. [CrossRef]
50. Brandolini, P.; Pepe, G.; Capolongo, D.; Cappadonia, C.; Cevasco, A.; Conoscenti, C.; Marsico, A.; Vergari, F.; Del Monte, M. Hillslope Degradation in Representative ITALIAN Areas: Just Soil Erosion Risk or Opportunity for Development? *Land Degrad. Dev.* **2018**, *29*, 3050–3068. [CrossRef]
51. Brunori, E.; Maesano, M.; Moresi, F.V.; Matteucci, G.; Biasi, R.; Scarascia Mugnozza, G. The Hidden Land Conservation Benefits of Olive-based (*Olea europaea* L.) Landscapes: An Agroforestry Investigation in the Southern Mediterranean (Calabria Region, Italy). *Land Degrad. Dev.* **2020**, *31*, 801–815. [CrossRef]
52. Sakellariou, M.; Psiloglou, B.E.; Giannakopoulos, C.; Mylona, P.V. Integration of Abandoned Lands in Sustainable Agriculture: The Case of Terraced Landscape Re-Cultivation in Mediterranean Island Conditions. *Land* **2021**, *10*, 457. [CrossRef]
53. Hurni, H.; Herweg, K.; Portner, B.; Liniger, H. Soil Erosion and Conservation in Global Agriculture. In *Land Use and Soil Resources*; Braimoh, A.K., Vlek, P.L.G., Eds.; Springer: Dordrecht, The Netherlands, 2008; pp. 41–71, ISBN 978-1-4020-6777-8.
54. Kiage, L.M. Perspectives on the Assumed Causes of Land Degradation in the Rangelands of Sub-Saharan Africa. *Prog. Phys. Geogr. Earth Environ.* **2013**, *37*, 664–684. [CrossRef]
55. Ochoa-Cueva, P.; Fries, A.; Montesinos, P.; Rodríguez-Díaz, J.A.; Boll, J. Spatial Estimation of Soil Erosion Risk by Land-cover Change in the Andes OF Southern Ecuador. *Land Degrad. Dev.* **2015**, *26*, 565–573. [CrossRef]
56. Bozzola, M.; Smale, M.; Di Falco, S. Climate, Shocks, Weather and Maize Intensification Decisions in Rural Kenya. In *Agricultural Adaptation to Climate Change in Africa*; Routledge: Abingdon, UK, 2018; pp. 107–128.
57. Chen, L.; Wei, W.; Fu, B.; Lü, Y. Soil and Water Conservation on the Loess Plateau in China: Review and Perspective. *Prog. Phys. Geogr. Earth Environ.* **2007**, *31*, 389–403. [CrossRef]
58. Fu, B.; Wang, S.; Liu, Y.; Liu, J.; Liang, W.; Miao, C. Hydrogeomorphic Ecosystem Responses to Natural and Anthropogenic Changes in the Loess Plateau of China. *Annu. Rev. Earth Planet. Sci.* **2017**, *45*, 223–243. [CrossRef]
59. Ge, J.; Pitman, A.J.; Guo, W.; Zan, B.; Fu, C. Impact of Revegetation of the Loess Plateau of China on the Regional Growing Season Water Balance. *Hydrol. Earth Syst. Sci.* **2020**, *24*, 515–533. [CrossRef]

60. Shitu, K.; Alzahrani, H.; Aslam, R.W. Modelling Sustainable Land Management Programme Intervention Effect on Soil Loss Rate in the Watershed Region. *Soil Use Manag.* **2025**, *41*, e70048. [CrossRef]
61. Abiye, W.; Waltner, I.; Kindie, H. Spatiotemporal Dynamics of Soil Erosion Response to Land Use Land Cover Dynamics and Climate Variability in Maybar Watershed, Awash Basin, Ethiopia. *Geol. Ecol. Landsc.* **2025**, *9*, 624–646. [CrossRef]
62. Mehta, D.; Caloiero, T.; Yadav, S.; Kumar, V. Rainfall Temporal Variability and Drought Analysis by Means of the Standardized Precipitation Index in Ganganagar District, Rajasthan, India. *Front. Clim.* **2025**, *7*, 1702356. [CrossRef]
63. Kumar, D.; Srivastav, S.S.; Pattnaik, S. Assessment of Solar and Wind Energy Potential in India in Recent Decades Using Benchmark Reanalysis Datasets. *Environ. Res. Clim.* **2025**, *5*, 015021. [CrossRef]
64. Khajuria, N.; Kaushik, S.P. Comprehensive Assessment of Land Use/Land Cover Transformations and Future Projections in a Semi-Arid Metropolitan City Utilising Artificial Neural Network- Based Cellular Automation. *J. Indian Soc. Remote Sens.* **2025**. [CrossRef]
65. Sharma, D.; Inbaraj, M.P.; Naz, A.; Chowdhury, A. Fate, Source Apportionment and Fractionation of Potentially Toxic Elements in Agricultural Soil around a Densely Populated, Semiarid Urban Center of India: Baseline Study and Ecological Risk Assessment. *Environ. Geochem. Health* **2024**, *46*, 207. [CrossRef]
66. Flores, B.M.; Staal, A.; Jakovac, C.C.; Hirota, M.; Holmgren, M.; Oliveira, R.S. Soil Erosion as a Resilience Drain in Disturbed Tropical Forests. *Plant Soil* **2020**, *450*, 11–25. [CrossRef]
67. Zeng, Z.; Estes, L.; Ziegler, A.D.; Chen, A.; Searchinger, T.; Hua, F.; Guan, K.; Jintrawet, A.; Wood, E.F. Highland Cropland Expansion and Forest Loss in Southeast Asia in the Twenty-First Century. *Nat. Geosci.* **2018**, *11*, 556–562. [CrossRef]
68. Harden, C.P. Interrelationships between Land Abandonment and Land Degradation: A Case from the Ecuadorian Andes. *Mt. Res. Dev.* **1996**, *16*, 274–280. [CrossRef]
69. Bajocco, S.; De Angelis, A.; Perini, L.; Ferrara, A.; Salvati, L. The Impact of Land Use/Land Cover Changes on Land Degradation Dynamics: A Mediterranean Case Study. *Environ. Manag.* **2012**, *49*, 980–989. [CrossRef]
70. Guns, M.; Vanacker, V. Forest Cover Change Trajectories and Their Impact on Landslide Occurrence in the Tropical Andes. *Environ. Earth Sci.* **2013**, *70*, 2941–2952. [CrossRef]
71. Bagwan, W.A.; Gavali, R.S. Delineating Changes in Soil Erosion Risk Zones Using RUSLE Model Based on Confusion Matrix for the Urmodi River Watershed, Maharashtra, India. *Model. Earth Syst. Environ.* **2021**, *7*, 2113–2126. [CrossRef]
72. Kumar, A.; Devi, M.; Deshmukh, B. Integrated Remote Sensing and Geographic Information System Based RUSLE Modelling for Estimation of Soil Loss in Western Himalaya, India. *Water Resour. Manage* **2014**, *28*, 3307–3317. [CrossRef]
73. Chinnasamy, P.; Honap, V.U.; Maske, A.B. Impact of 2018 Kerala Floods on Soil Erosion: Need for Post-Disaster Soil Management. *J. Indian Soc. Remote Sens* **2020**, *48*, 1373–1388. [CrossRef]
74. Dregne, H.E. Land Degradation in the Drylands. *Arid. Land Res. Manag.* **2002**, *16*, 99–132. [CrossRef]
75. Byrd, K.B.; Flint, L.E.; Alvarez, P.; Casey, C.F.; Sleeter, B.M.; Soulard, C.E.; Flint, A.L.; Sohl, T.L. Integrated Climate and Land Use Change Scenarios for California Rangeland Ecosystem Services: Wildlife Habitat, Soil Carbon, and Water Supply. *Landsc. Ecol.* **2015**, *30*, 729–750. [CrossRef]
76. Edwards, B.L.; Webb, N.P.; Brown, D.P.; Elias, E.; Peck, D.E.; Pierson, F.B.; Williams, C.J.; Herrick, J.E. Climate Change Impacts on Wind and Water Erosion on US Rangelands. *J. Soil Water Conserv.* **2019**, *74*, 405–418. [CrossRef]
77. Pradeep, G.S.; Krishnan, M.V.N.; Vijith, H. Identification of Critical Soil Erosion Prone Areas and Annual Average Soil Loss in an Upland Agricultural Watershed of Western Ghats, Using Analytical Hierarchy Process (AHP) and RUSLE Techniques. *Arab. J. Geosci.* **2015**, *8*, 3697–3711. [CrossRef]
78. Kijowska-Strugała, M.; Bucała-Hrabia, A.; Demczuk, P. Long-term Impact of Land Use Changes on Soil Erosion in an Agricultural Catchment (in the Western Polish Carpathians). *Land Degrad. Dev.* **2018**, *29*, 1871–1884. [CrossRef]
79. Harden, C.P. Soil Erosion and Sustainable Mountain Development. *Mt. Res. Dev.* **2001**, *21*, 77–83. [CrossRef]
80. Naqvi, S.A.A.; Tariq, A.; Shahzad, M.; Khalid, S.; Tariq, Z.; Salma, U.; Haseeb, M.; Soufan, W. Predicting Soil Erosion Risk Using the Revised Universal Soil Loss Equation (RUSLE) Model and Geo-spatial Methods. *Hydrol. Process.* **2024**, *38*, e15248. [CrossRef]
81. Guo, Z.; Huang, N.; Dong, Z.; Van Pelt, R.S.; Zobeck, T.M. Wind Erosion Induced Soil Degradation in Northern China: Status, Measures and Perspective. *Sustainability* **2014**, *6*, 8951–8966. [CrossRef]
82. Petrosillo, I.; Valente, D.; Scavuzzo, C.M.; Selvan, T. Land Degradation Pattern and Ecosystem Services. *Front. Environ. Sci.* **2023**, *11*, 1137768. [CrossRef]
83. Sun, X.; Li, G.; Wu, Q.; Li, D.; Lu, D. Examining the Effects of Soil and Water Conservation Measures on Patterns and Magnitudes of Vegetation Cover Change in a Subtropical Region Using Time Series Landsat Imagery. *Remote Sens.* **2024**, *16*, 714. [CrossRef]
84. Paul, S.S.; Li, J.; Li, Y.; Shen, L. Assessing Land Use–Land Cover Change and Soil Erosion Potential Using a Combined Approach through Remote Sensing, RUSLE and Random Forest Algorithm. *Geocarto Int.* **2021**, *36*, 361–375. [CrossRef]

85. Kumar, S.; Kushwaha, S.P.S. Modelling Soil Erosion Risk Based on RUSLE-3D Using GIS in a Shivalik Sub-Watershed. *J. Earth Syst. Sci.* **2013**, *122*, 389–398. [CrossRef]
86. Mallick, J.; Alashker, Y.; Mohammad, S.A.-D.; Ahmed, M.; Hasan, M.A. Risk Assessment of Soil Erosion in Semi-Arid Mountainous Watershed in Saudi Arabia by RUSLE Model Coupled with Remote Sensing and GIS. *Geocarto Int.* **2014**, *29*, 915–940. [CrossRef]